

THE DEVELOPMENT OF A CORRELATION FOR DETERMINING
OIL DENSITY IN HIGH TEMPERATURE RESERVOIRS

A Thesis

by

Thurman William Witte Jr.

Submitted to the Graduate College of
Texas A&M University
in partial fulfillment of the requirements for the degree of
MASTER OF SCIENCE

December 1987

Major Subject: Petroleum Engineering


THE DEVELOPMENT OF A CORRELATION FOR DETERMINING
OIL DENSITY IN HIGH TEMPERATURE RESERVOIRS

A Thesis

by

Thurman William Witte Jr.

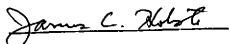
Approved as to style and content by:



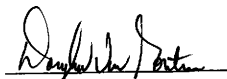
James W. Jennings
(Chair of Committee)



Larry D. Piper
(Member)



James C. Holste
(Member)



W. Douglas Von Gonten
(Head of Department)

December 1987

ABSTRACT

The Development of a Correlation for Determining Oil Density in High Temperature Reservoirs. (December 1987)
Thurman William Witte, Jr., B.S. Colorado School of Mines
Chairman of Advisory Committee: Dr. James W. Jennings

This study presents a correlation for estimation of liquid density from oil composition using ideal solution principles. The present method, developed by Standing in the early 1940's, is inaccurate at low fluid densities and high reservoir temperatures. The correlation developed in this study overcomes these difficulties.

The new correlation includes a more accurate equation for the effect of thermal expansion on fluid density, a new pseudoliquid density equation which accounts for the increased quantities of methane and ethane found in reservoir fluids of low density, and a new correction for non-hydrocarbon components.

The correlations were developed using non-linear regression methods on laboratory data from 1310 reservoir fluid samples.

DEDICATION

This thesis is dedicated to the following people who have been very important in my life:

My daughter Audrey who has brought me great joy and who makes being a father very enjoyable;

My parents for their continual encouragement to better myself personally and professionally;

My many friends who I have had the great fortune of becoming acquainted with, and the many enjoyable times I have spent with them while at A&M;

And above all to God who helped me continue when it appeared to be impossible to do so.

ACKNOWLEDGEMENTS

The author wishes to thank the following individuals for their contributions to this work:

Dr. William D. McCain, Jr., for his encouragement and guidance during this research;

Dr. L. D. Piper for his helpful suggestions during this research;

My fellow graduate students who had some very useful suggestions pertaining to this research; and

Drs. J. W. Jennings, L. D. Piper, and J. C. Holste for serving as members of the authors committee.

TABLE OF CONTENTS

	Page
ABSTRACT	iii
DEDICATION	iv
ACKNOWLEDGMENTS	v
TABLE OF CONTENTS	vi
LIST OF FIGURES	vii
LIST OF TABLES	xii
INTRODUCTION	1
REVIEW OF LITERATURE	3
IDEAL SOLUTION THEORY	5
DATA BASE DEVELOPMENT	12
ANALYSIS OF DATA AND DEVELOPMENT OF EQUATIONS	15
CORRECTION TO DENSITY DUE TO THERMAL EXPANSION	15
CALCULATION OF PSEUDOLIQUID DENSITY FROM COMPOSITION	25
NON-HYDROCARBON CORRECTIONS TO THE NEW DENSITY CORRELATION	71
Correction to Pseudoliquid Density Due to Non-Hydrocarbon Components	71
Final Corrections to the New Density Correlation Due to the Affects of Non-Hydrocarbon Components	82
SUMMARY AND CONCLUSIONS	90
NOMENCLATURE	93
REFERENCES	94
APPENDIX A - NEW PROCEDURE FOR CALCULATING LIQUID DENSITY AT RESERVOIR CONDITIONS	95
VITA	99

LIST OF FIGURES

Figure	Page
1 - VARIATION OF APPARENT DENSITY OF METHANE AND ETHANE WITH DENSITY OF THE SYSTEM	8
2 - STANDING'S DENSITY CORRECTION FOR THE THERMAL EXPANSION OF LIQUIDS	16
3 - ISOMETRIC PRESSURE-TEMPERATURE DIAGRAM SHOWING THE STEPS IN CALCULATING LIQUID DENSITY AT BUBBLE POINT PRESSURE AND 60°F.	19
4 - NEW DENSITY CORRECTION FOR THE THERMAL EXPANSION OF LIQUIDS	23
5 - COMPARISON OF THE DENSITY CORRECTION FOR THE THERMAL EXPANSION OF LIQUIDS CALCULATED FROM THE NEW EQUATION VERSUS THE ACTUAL CORRECTION (SAMPLES WITH LOW CONCENTRATIONS OF NON-HYDROCARBONS)	26
6 - COMPARISON OF THE DENSITY CORRECTION FOR THE THERMAL EXPANSION OF LIQUIDS CALCULATED FROM THE STANDING EQUATION VERSUS THE ACTUAL CORRECTION (SAMPLES WITH LOW CONCENTRATIONS OF NON-HYDROCARBONS)	27
7 - COMPARISON OF THE DENSITY CORRECTION FOR THE THERMAL EXPANSION OF LIQUIDS CALCULATED FROM THE NEW EQUATION VERSUS THE ACTUAL CORRECTION (ALL SAMPLES)	28
8 - COMPARISON OF THE DENSITY CORRECTION FOR THE THERMAL EXPANSION OF LIQUIDS CALCULATED FROM THE STANDING EQUATION VERSUS THE ACTUAL CORRECTION (ALL SAMPLES)	29
9 - RESIDUAL IN THE PREDICTED DENSITY CORRECTION FOR THE THERMAL EXPANSION OF LIQUIDS VERSUS RESERVOIR TEMPERATURE (ALL SAMPLES)	30
10 - RESIDUAL IN THE PREDICTED DENSITY CORRECTION FOR THE THERMAL EXPANSION OF LIQUIDS VERSUS RESERVOIR FLUID DENSITY (ALL SAMPLES)	31

LIST OF FIGURES CONTINUED

Figure	Page
11 - COMPARISON OF THE RESERVOIR FLUID DENSITY CALCULATED FROM STANDING'S CORRELATION USING THE NEW EQUATION FOR THE THERMAL EXPANSION CORRECTION VERSUS THE ACTUAL RESERVOIR FLUID DENSITY	32
12 - COMPARISON OF THE RESERVOIR FLUID DENSITY CALCULATED FROM STANDING'S CORRELATION WITHOUT ANY MODIFICATIONS VERSUS THE ACTUAL RESERVOIR FLUID DENSITY	33
13 - CALCULATED APPARENT DENSITY OF ETHANE (EQS. 9 & 23) VERSUS PSEUDOLIQUID DENSITY OF THE MIXTURE	37
14 - VOLUME OF THE PROPANE PLUS FRACTION VERSUS VOLUME OF THE MIXTURE (ALL SAMPLES)	40
15 - VOLUME OF THE PROPANE PLUS FRACTION VERSUS VOLUME OF THE MIXTURE (SAMPLES WITH LOW CONCENTRATIONS OF NON-HYDROCARBONS)	41
16 - RATIO OF THE VOLUME OF LIGHT COMPONENTS TO THE MIXTURE VOLUME VERSUS THE WEIGHT FRACTION OF METHANE IN THE MIXTURE (SAMPLES WITH LOW CONCENTRATIONS OF NON-HYDROCARBONS)	44
17 - RATIO OF THE VOLUME OF LIGHT COMPONENTS TO THE MIXTURE VOLUME VERSUS THE WEIGHT FRACTION OF ETHANE IN THE MIXTURE (SAMPLES WITH LOW CONCENTRATIONS OF NON-HYDROCARBONS)	45
18 - RATIO OF THE VOLUME OF LIGHT COMPONENTS TO THE PROPANE PLUS VOLUME VERSUS THE WEIGHT RATIO OF METHANE TO PROPANE PLUS (SAMPLES WITH LOW CONCENTRATIONS OF NON-HYDROCARBONS)	46
19 - RATIO OF THE VOLUME OF LIGHT COMPONENTS TO THE PROPANE PLUS VOLUME VERSUS THE WEIGHT RATIO OF ETHANE TO PROPANE PLUS (SAMPLES WITH LOW CONCENTRATIONS OF NON-HYDROCARBONS)	47
20 - PREDICTED VOLUME OF THE MIXTURE FROM EQ. 30 VERSUS THE ACTUAL VOLUME OF THE MIXTURE (SAMPLES WITH LOW CONCENTRATIONS OF NON-HYDROCARBONS)	51

LIST OF FIGURES CONTINUED

Figure	Page
21 - RESIDUALS OF THE PREDICTED VOLUME VERSUS THE VOLUME OF THE MIXTURE (SAMPLES WITH LOW CONCENTRATIONS OF NON-HYDROCARBONS)	52
22 - RESIDUALS OF THE PREDICTED VOLUME VERSUS THE METHANE WEIGHT FRACTION TERM (SAMPLES WITH LOW CONCENTRATIONS OF NON-HYDROCARBONS)	53
23 - RESIDUALS OF THE PREDICTED VOLUME VERSUS THE ETHANE WEIGHT FRACTION TERM (SAMPLES WITH LOW CONCENTRATIONS OF NON-HYDROCARBONS)	54
24 - RESIDUALS OF THE PREDICTED VOLUME VERSUS THE PROPANE PLUS WEIGHT FRACTION TERM (SAMPLES WITH LOW CONCENTRATIONS OF NON-HYDROCARBONS)	55
25 - PREDICTED VOLUME OF THE MIXTURE FROM EQ. 30 VERSUS THE ACTUAL VOLUME OF THE MIXTURE AFTER REMOVAL OF OUTLIERS (SAMPLES WITH LOW CONCENTRATIONS OF NON-HYDROCARBONS)	56
26 - RESIDUALS OF THE PREDICTED VOLUME VERSUS THE VOLUME OF THE MIXTURE AFTER REMOVAL OF OUTLIERS (SAMPLES WITH LOW CONCENTRATIONS OF NON-HYDROCARBONS)	57
27 - RESIDUALS OF THE PREDICTED VOLUME VERSUS THE METHANE WEIGHT FRACTION TERM AFTER REMOVAL OF OUTLIERS (SAMPLES WITH LOW CONCENTRATIONS OF NON-HYDROCARBONS)	58
28 - RESIDUALS OF THE PREDICTED VOLUME VERSUS THE ETHANE WEIGHT FRACTION TERM AFTER REMOVAL OF OUTLIERS (SAMPLES WITH LOW CONCENTRATIONS OF NON-HYDROCARBONS)	59
29 - RESIDUALS OF THE PREDICTED VOLUME VERSUS THE PROPANE PLUS WEIGHT FRACTION TERM AFTER REMOVAL OF OUTLIERS (SAMPLES WITH LOW CONCENTRATIONS OF NON-HYDROCARBONS)	60
30 - PREDICTED VOLUME OF THE MIXTURE FROM EQ. 31 VERSUS THE ACTUAL VOLUME OF THE MIXTURE AFTER REMOVAL OF OUTLIERS (SAMPLES WITH LOW CONCENTRATIONS OF NON-HYDROCARBONS)	63
31 - RESIDUALS OF THE PREDICTED VOLUME VERSUS THE VOLUME OF THE MIXTURE AFTER REMOVAL OF OUTLIERS (SAMPLES WITH LOW CONCENTRATIONS OF NON-HYDROCARBONS)	64

LIST OF FIGURES CONTINUED

Figure	Page
32 - RESIDUALS OF THE PREDICTED VOLUME VERSUS THE METHANE WEIGHT FRACTION TERM AFTER REMOVAL OF OUTLIERS (SAMPLES WITH LOW CONCENTRATIONS OF NON-HYDROCARBONS)	65
33 - RESIDUALS OF THE PREDICTED VOLUME VERSUS THE ETHANE WEIGHT FRACTION TERM AFTER REMOVAL OF OUTLIERS (SAMPLES WITH LOW CONCENTRATIONS OF NON-HYDROCARBONS)	66
34 - PREDICTED PSEUDOLIQUID DENSITY FROM THE MODEL (EQ. 33) VERSUS THE RESERVOIR FLUID DENSITY REFERRED TO STANDARD CONDITIONS (SAMPLES WITH LOW CONCENTRATIONS OF NON-HYDROCARBONS)	68
35 - RESIDUALS OF THE PREDICTED PSEUDOLIQUID DENSITY VERSUS THE RESERVOIR FLUID DENSITY REFERRED TO STANDARD CONDITIONS (SAMPLES WITH LOW CONCENTRATIONS OF NON-HYDROCARBONS)	69
36 - PREDICTED VOLUME OF THE MIXTURE FROM EQ. 34 VERSUS THE ACTUAL VOLUME OF THE MIXTURE (ALL SAMPLES)	75
37 - RESIDUALS OF THE PREDICTED VOLUME VERSUS THE VOLUME OF THE MIXTURE (ALL SAMPLES)	76
38 - RESIDUALS OF THE PREDICTED VOLUME VERSUS THE METHANE WEIGHT FRACTION TERM (ALL SAMPLES)	77
39 - RESIDUALS OF THE PREDICTED VOLUME VERSUS THE ETHANE WEIGHT FRACTION TERM (ALL SAMPLES)	78
40 - PREDICTED PSEUDOLIQUID DENSITY FROM THE MODEL WHICH ACCOUNTS FOR NON-HYDROCARBONS (EQ. 35) VERSUS THE RESERVOIR FLUID DENSITY REFERRED TO STANDARD CONDITIONS (ALL SAMPLES)	80
41 - RESIDUALS OF THE PREDICTED PSEUDOLIQUID DENSITY VERSUS THE RESERVOIR FLUID DENSITY REFERRED TO STANDARD CONDITIONS (ALL SAMPLES)	81
42 - PREDICTED RESERVOIR FLUID DENSITY FROM THE NEW CORRELATION BEFORE FINAL NON-HYDROCARBON CORRECTIONS VERSUS THE ACTUAL RESERVOIR FLUID DENSITY (ALL SAMPLES)	83

LIST OF FIGURES CONTINUED

Figure	Page
43 - RESIDUALS FROM THE PREDICTED RESERVOIR FLUID DENSITY BEFORE FINAL NON-HYDROCARBON CORRECTIONS VERSUS THE WEIGHT FRACTION OF CARBON DIOXIDE IN THE MIXTURE (ALL SAMPLES)	84
44 - RESIDUALS FROM THE PREDICTED RESERVOIR FLUID DENSITY BEFORE FINAL NON-HYDROCARBON CORRECTIONS VERSUS THE WEIGHT FRACTION OF HYDROGEN SULFIDE IN THE MIXTURE (ALL SAMPLES)	85
45 - RESIDUALS FROM THE PREDICTED RESERVOIR FLUID DENSITY BEFORE FINAL NON-HYDROCARBON CORRECTIONS VERSUS THE WEIGHT FRACTION OF NITROGEN IN THE MIXTURE (ALL SAMPLES)	86
46 - PREDICTED RESERVOIR FLUID DENSITY FROM THE FINAL FORM OF THE NEW CORRELATION VERSUS THE ACTUAL RESERVOIR FLUID DENSITY (ALL SAMPLES)	88
47 - RESIDUALS FROM THE PREDICTED RESERVOIR FLUID DENSITY VERSUS THE ACTUAL RESERVOIR FLUID DENSITY (ALL SAMPLES)	89

LIST OF TABLES

Table	Page
1 - RANGES OF DATA	14
2 - PARAMETERS FOR THE NEW EQUATION FOR THE THERMAL EXPANSION OF LIQUIDS	21
3 - ACCURACY OF THE NEW EQUATION FOR THE THERMAL EXPANSION OF LIQUIDS	22
4 - PARAMETERS FOR THE PSEUDOLIQUID DENSITY MODEL WITHOUT NON-HYDROCARBONS	70
5 - CRITICAL PROPERTIES AND MOLECULAR WEIGHTS FOR THE LIGHTER HYDROCARBONS AND NON-HYDROCARBON COMPONENTS	72
6 - PARAMETERS FOR THE PSEUDOLIQUID DENSITY MODEL WHICH INCLUDES THE AFFECTS OF NON-HYDROCARBONS	74
7 - SUMMARY OF IMPROVEMENTS IN OBTAINING THE NEW RESERVOIR FLUID DENSITY CORRELATION	92

INTRODUCTION

The density of a reservoir liquid at reservoir conditions and surface conditions is necessary when making vapor liquid equilibria calculations. Formation volume factors and gas-oil ratios are determined from the oil density when using these calculations. In addition to vapor liquid equilibria calculations, computer based compositional simulators require density information.

Liquid density can be obtained experimentally or estimated. At the surface it is usually measured. At reservoir conditions it is normally estimated using information readily measured at the surface. Some of the methods of estimating liquid density at reservoir conditions are from the composition of the reservoir liquid, from an equation of state, or from surface measurements consisting of gas-oil ratio, dissolved gas gravity, tank oil specific gravity and temperature. The density determined from a reservoir fluid study is the most accurate, but the expense involved may prohibit its use in addition to the inadequacy of this data for a compositional simulator where the oil density will be changing. Compositional simulation is necessary for reservoir fluids which experience a change in composition as the fluids are produced. In general compositional simulators make use of equations of state for determining densities of the liquid and gas phases present in the reservoir. Equations of state provide fairly accurate gas densities, but usually are not very

This thesis follows the style of the Journal of Petroleum Technology

accurate for liquid densities. This is particularly true near the critical point on the phase envelope, which is where reservoir fluids with low densities generally lie. The density from surface measurements presents the problem of time under production in order to gather the necessary data. The best choice for determining density to be used in compositional simulation is the method using the composition of the oil since the composition for a volatile oil will change during the depletion of the reservoir.

With the current state of technology in the petroleum industry reservoirs are being discovered at very great depths with temperatures frequently in excess of 200 °F. In many instances the fluids being found in these reservoirs are volatile oils with low densities. The greatest benefit will be with a correlation which applies to volatile oils and also high temperature reservoirs. The presently used correlation was developed in the 1940's by Standing. His correlation determines oil density from the composition of the oil, however, the density predicted in high temperature reservoirs ($T > 200^\circ\text{F}$) and for fluids with low density ($\rho < 40$ lb/cu ft) can be seriously in error.

The purpose of this study is to obtain an improved correlation for oil density which encompasses the full range of oil density over an expanded temperature range. In addition, non-hydrocarbon components will be included in the correlation to further improve the accuracy.

REVIEW OF LITERATURE

Several methods of estimating liquid density at reservoir conditions are available in the literature. This review will concentrate on the application of ideal solution principles to calculate liquid density from its composition.

Katz¹ presented a method of calculating density from composition using ideal solution theory and the concept of apparent liquid densities for methane and ethane. A revision was made to the apparent density functions by Standing and Katz², due to inaccuracies in the apparent densities used by Katz in his previous work. The results of this work were published in graphical form. The range of densities presented were from 0.5 gm/cc to 0.95 gm/cc with a maximum weight percent for methane of 24 percent. Hanson, et al³ presented a correlation with an increased range of densities (0.3 gm/cc-1.0 gm/cc) and concentrations of methane up to 35 percent methane by weight.

Sage, et al⁴ presented data on the effect of pressure and temperature on the density of liquids. Standing and Katz² used their data, and other data appearing in the literature, to produce graphical correlations showing the effect of pressure on liquid densities at 60°F and of temperature on liquid densities at elevated pressures. The range of applicability for these two correlations was densities between 0.6 gm/cc and 0.9 gm/cc, pressures to 10,000 psi, and temperatures to 240°F. Brown, et al⁵ presented a modification to the pressure correction figure increasing the pressure range to 15,000 psi.

Standing⁶ published a compilation of the previous work on calculating densities from ideal solution theory and also provided equations for the pseudoliquid density, pressure correction and temperature correction figures. The GPSA Engineering Data Book⁷ presented a method of including non-hydrocarbon components in the density calculation.

IDEAL SOLUTION THEORY

The development of the equations for determining the liquid density of a mixture used in this study relies on ideal solution theory. This theory dictates that there is no change in total volume when two or more components are mixed, i.e. a unit volume of one liquid added to a unit volume of another liquid will result in two volumes of mixture. The following equation describes this:

$$V_m = V_1 + V_2 \dots \dots \dots (1)$$

To determine the density of the mixture the following equation is used:

$$\rho_m = \frac{W_1 + W_2}{V_1 + V_2} \dots \dots \dots (2)$$

Expanding this equation to a mixture of N components yields:

$$\rho_m = \frac{\sum_{j=1}^N W_j}{\sum_{j=1}^N V_j} \dots \dots \dots (3)$$

The typical method of reporting the composition for an oil sample is on a mole percent basis. The following set of equations, in addition

to Eq. 3, are used to determine the density of a liquid mixture at standard conditions of 14.7 psia and 60°F:

$$W_j = x_j M_j \quad \dots \dots \dots (4)$$

$$V_j = x_j M_j / \rho_j \quad \dots \dots \dots (5)$$

The molecular weights and densities of the individual components can be found in readily available sources such as the GPSA Engineering Databook⁷.

One problem that arises when using ideal solution theory in determining the liquid density of hydrocarbon mixtures containing methane and ethane is: methane and ethane do not exist as liquids at standard conditions and thus have no associated liquid density at standard conditions. Standing and Katz² overcame this limitation by introducing the concept of apparent liquid density for methane and ethane. Standing and Katz performed laboratory experiments on binary mixtures of methane and hydrocarbons heavier than ethane and also mixtures of ethane and hydrocarbons heavier than ethane. The apparent liquid densities of methane and ethane were calculated using the following equations which come from ideal solution theory:

$$\rho_{a,c_1} = \frac{x_{c_1} M_{c_1}}{\frac{x_{c_1} M_{c_1} + x_{\text{comp } 2} M_{\text{comp } 2}}{\rho_{\text{binary}}} - \frac{x_{\text{comp } 2} M_{\text{comp } 2}}{\rho_{\text{comp } 2}}} \quad \dots (6)$$

$$\rho_{a,c_2} = \frac{x_{c_2} M_{c_2}}{\frac{x_{c_2} M_{c_2} + x_{\text{comp } 2} M_{\text{comp } 2}}{\rho_{\text{binary}}} - \frac{x_{\text{comp } 2} M_{\text{comp } 2}}{\rho_{\text{comp } 2}}} \quad \dots (7)$$

Fig. 1 is reproduced from Standing and Katz's publication concerning this work. This figure shows that the apparent densities of methane and ethane are functions of the total system density. The following equations were determined from the work done by Standing and Katz:

$$\rho_{a,c_1} = 0.312 + 0.450 \rho_{c_1+} \quad \dots \dots \dots (8)$$

$$\rho_{a,c_2} = 15.3 + 0.3167 \rho_{c_2+} \quad \dots \dots \dots (9)$$

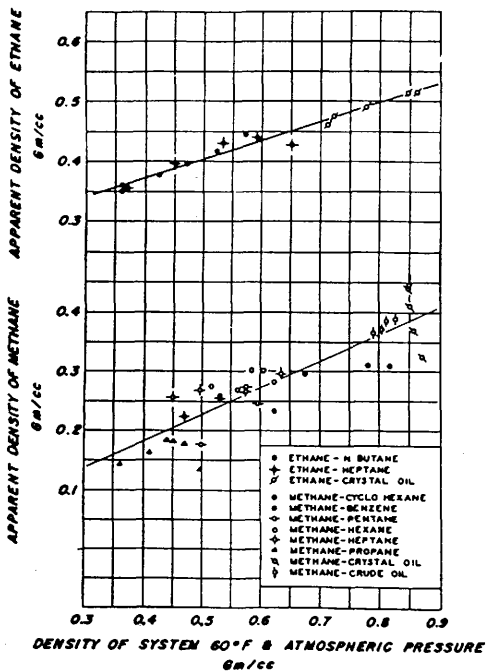


FIGURE 1 - VARIATION OF APPARENT DENSITY OF METHANE AND ETHANE WITH DENSITY OF THE SYSTEM

Eqs. 8 and 9 cannot be used directly in calculating the density of a mixture, but by making a slight modification to Eq. 3 and with algebraic manipulation the density of the ethane plus portion of the mixture can be calculated. From this the density of the mixture can be calculated. The following equations show this:

$$\begin{aligned} \rho_{C_2+} &= \frac{\sum_{j=C_2}^N W_j}{\sum_{j=C_2}^N V_j} = \frac{\sum_{j=C_2}^N x_j M_j}{\sum_{j=C_2}^N x_j M_j / \rho_j} \\ &= \frac{\sum_{j=C_2}^N x_j M_j}{\frac{x_{C_2} M_{C_2}}{\rho_{C_2}} + \sum_{j=C_3}^N x_j M_j / \rho_j} \\ &= \frac{\sum_{j=C_2}^N x_j M_j}{\frac{x_{C_2} M_{C_2}}{15.3 + 0.3167 \rho_{C_2+}} + \sum_{j=C_3}^N x_j M_j / \rho_j} \end{aligned}$$

rearrangement yields:

$$\begin{aligned}
 & (0.3167 \sum_{j=c_2}^N x_j M_j / \rho_j) \rho_{c_2}^2 \\
 & + (x_{c_1} M_{c_2} - 0.3167 \sum_{j=c_2}^N x_j M_j + 15.3 \sum_{j=c_2}^N x_j M_j / \rho_j) \rho_{c_2} \\
 & - 15.3 \sum_{j=c_2}^N x_j M_j = 0 \dots \dots \dots (10)
 \end{aligned}$$

Simplification of the summation terms results in:

$$\begin{aligned}
 & (0.3167 V_{c_2} \rho_{c_2}^2 + (W_{c_2} - 0.3167 W_{c_2} + 15.3 V_{c_2}) \rho_{c_2} \\
 & - 15.3 W_{c_2} = 0 \dots \dots \dots (11)
 \end{aligned}$$

Since the form of this equation is quadratic the density of C_2^+ can be calculated directly. From this value the apparent density of ethane can be calculated using Eq. 9. The development of the equation for C_1^+ is similar to the previous development for C_2^+ .

The final quadratic equation is:

$$(0.450 V_{C_1+}) \rho_{C_1+}^2 + (W_{C_1} - 0.450 W_{C_1+} + 0.312 V_{C_1+}) \rho_{C_1+} - 0.312 W_{C_1+} = 0 \quad \dots \dots \dots (12)$$

The pseudoliquid density of the mixture can therefore be calculated from Eq. 12.

DATA BASE DEVELOPMENT

The data base used in obtaining an improved density correlation consists of data from studies on reservoir fluid samples from throughout the world. A total of 1310 reservoir fluid studies were available for analysis. The data from each reservoir fluid study was input into a computer data base. The data included in the data base consists of:

1. Sample reference number
2. PVT data
 - bubble point pressure of the sample
 - reservoir temperature
 - specific volume of the sample
 - thermal expansion
 - final temperature of thermal expansion
 - pressure at which the thermal expansion
was conducted under
 - relative volume at thermal expansion pressure
3. Composition of sample (mole percent basis)
 - hydrogen sulfide
 - carbon dioxide
 - nitrogen
 - methane
 - ethane
 - propane

iso-butane
normal-butane
iso-pentane
normal-pentane
hexane
heptanes and heavier
density of the heptanes and heavier fraction
molecular weight of the heptanes and heavier fraction

The ranges of data for the reservoir fluid samples and the number of samples used in each step of the correlation development are summarized in Table 1.

TABLE 1
RANGES OF DATA

	Total	With Limits on Non-hydrocarbons
Number of reservoir fluid analyses	1310	
Number of reservoir fluid analyses used in the thermal expansion correlation	1096	430
Number of reservoir fluid analyses used in the pseudoliquid density correlation	1248	544
Number of reservoir fluid analyses used in the non-hydrocarbon correlation	766	
Bubble point pressure	35	to 10115 psia
Reservoir temperature	60	to 355 °F
Reservoir fluid density	24.4	to 60.31 lb/cu ft
Mole percent methane	0	to 80.07
Mole percent ethane	0	to 25.89
Mole percent carbon dioxide	0	to 66.97
Mole percent hydrogen sulfide	0	to 35.26
Mole percent nitrogen	0	to 43.10

ANALYSIS OF DATA AND DEVELOPMENT OF EQUATIONS

The analysis used Standing's correlation as a starting point. The development of the density correlation was split into three parts. The first of these was the correction to density due to thermal expansion. The second was the development of an equation to determine pseudoliquid density from the composition of a reservoir fluid. Finally corrections to density due to the quantity of CO_2 , H_2S and N_2 were developed.

CORRECTION TO DENSITY DUE TO THERMAL EXPANSION

In developing the correlation for the 'Correction to Density Due to Thermal Expansion' the figure and equation presented by Standing⁶ were used as a model. This figure is reproduced from the equation given by Standing⁶ and is shown here as Fig. 2. Three parameters are shown on this figure:

1. density at bubble point pressure and 60 °F, ρ_{bs}
2. change in density when the temperature is raised from 60 °F to reservoir temperature, $\Delta\rho_T$,
and
3. reservoir temperature, T_R .

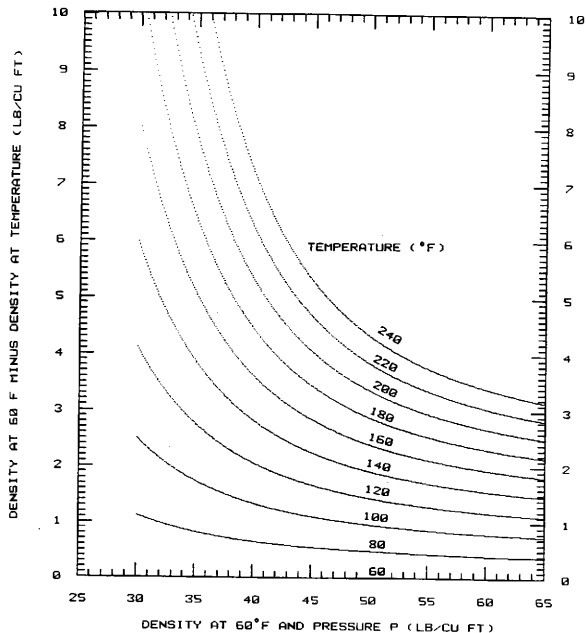


FIGURE 2 - STANDING'S DENSITY CORRECTION FOR THE THERMAL EXPANSION OF LIQUIDS

1. The following algorithm was used in determining the density at bubble point pressure and 60 °F using PVT data from the reservoir fluid analyses. A single subscript in the following equations indicates the conditions of pressure and temperature, while two subscripts are used for the conditions of pressure and temperature respectively. Fig. 3 shows the information which is calculated from each step.

- a. Density at Thermal Expansion Pressure and Laboratory Temperature:

$$\rho_e = \frac{(V/V_e)_T}{(V/V_b)_p} \left(\frac{1}{v_b} \right) \dots \dots \dots (13)$$

- b. Density at Thermal Expansion Pressure and 60 °F.

This is an iterative procedure using Standing's equation for the density correction for the thermal expansion of liquids (an assumption is made that this equation is accurate at low temperatures):

$$\Delta\rho_1 = [0.0133 + 152.4(\rho_e + \Delta\rho_1)^{-2.45}]_{(T_e-60)}$$

$$- [(8.1 \times 10^{-6}) - 0.0622 \{10^{-0.0764(\rho_e + \Delta\rho_1)}\}]_{(T_e-60)}^2 \dots (14)$$

$$\rho_{es} = \rho_e + \Delta\rho_1 \dots \dots \dots (15)$$

- c. Density at 14.7 psia and 60 °F

This is also an iterative procedure using Standing's equation for the density correction for compressibility of liquids (an assumption is made that this equation is correct over the entire pressure range)

$$\Delta\rho_2 = [0.167 + 16.181(10^{-0.0425(\rho_{es} - \Delta\rho_2)})](p_e/1000) \\ - 0.01[0.299+263(10^{-0.0603(\rho_{es} - \Delta\rho_2)})](p_e/1000)^2 \dots (16)$$

$$\rho_{sc} = \rho_{es} - \Delta\rho_2 \dots (17)$$

- d. Density at bubble point pressure and 60 °F

$$\Delta\rho_p = [0.167+16.181(10^{-0.0425\rho_{sc}})](p_b/1000) \\ - 0.01[0.299+263(10^{-0.0603\rho_{sc}})](p_b/1000)^2 \dots (18)$$

$$\rho_{bs} = \rho_{sc} + \Delta\rho_p \dots (19)$$

2. The change in density was calculated from the following equation:

$$\Delta\rho_T = \rho_{bs} - \rho_b \dots \dots \dots (20)$$

3. The reservoir temperature, T_R , was taken directly from the data base.

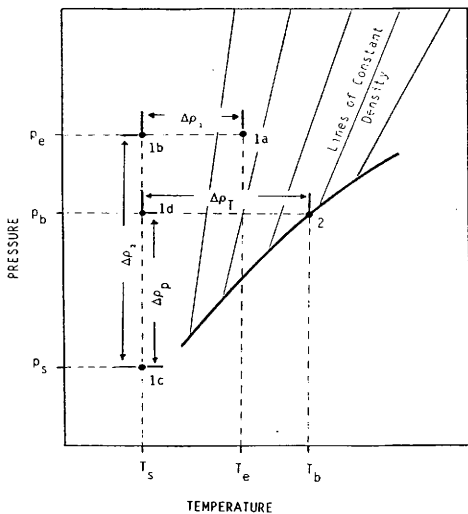


FIGURE 3 - ISOMETRIC PRESSURE-TEMPERATURE DIAGRAM SHOWING THE STEPS IN CALCULATING LIQUID DENSITY AT BUBBLE POINT PRESSURE AND 60°F.

A total of 1310 reservoir fluid samples were available in the data base, however only 1096 of the samples had the data necessary to determine the density at bubble point pressure and 60°F, and the change in density from 60°F to reservoir temperature. Statistics were calculated on the set of three values (ρ_{bs} , $\Delta\rho_T$, and T_R) from the 1096 reservoir fluid samples in an attempt to fit the data to an equation taking the same form as Standing's equation for the "Density Correction for the Thermal Expansion of Liquids." The form of this equation is:

$$\Delta\rho_T = [a_1 + a_2(\rho_{bs})^{a_3}](T_R - 60)^{a_4} + [a_5 + a_6(10^{a_7 \rho_{bs}})](T_R - 60)^{a_8} \dots \dots \dots (21)$$

An acceptable fit could not be obtained with the entire data set. It was found however, that by eliminating the samples with high quantities of non-hydrocarbon components from the statistical analysis, an acceptable fit could be obtained. The limits placed on the non-hydrocarbon components were $H_2S < 1.0$ mole percent, $CO_2 < 1.0$ mole percent, $N_2 < 1.0$ mole percent and total non-hydrocarbons < 2.0 mole percent. There were a total of 430 samples used in the analysis

after the samples with high non-hydrocarbon concentrations were removed. Table 2 shows the resultant parameters obtained for the thermal expansion correction equation.

TABLE 2
PARAMETERS FOR THE NEW EQUATION FOR THE THERMAL EXPANSION OF LIQUIDS

<u>Parameter</u>	<u>Value</u>
a_1	0.00302
a_2	1.505
a_3	-0.951
a_4	0.938
a_5	-0.0216
a_6	0.0233
a_7	-0.0161
a_8	0.475

Replacing the parameters in Eq. 21 with these values yields the final form of the thermal expansion equation:

$$\Delta\rho_T = [0.00302 + 1.505(\rho_{bs})^{-0.951}](T_R-60)^{0.938} \\ + [-0.0216 + 0.0233(10^{-0.0161\rho_{bs}})](T_R-60)^{0.475} \dots (22)$$

Fig. 4 shows the graphical representation of this equation. Table 3 gives statistical information on the accuracy of the resultant equation.

TABLE 3

ACCURACY OF THE NEW EQUATION FOR THE THERMAL EXPANSION OF LIQUIDS

	RANGE OF ERROR FOR $\Delta\rho_T$		Average
	Minimum Deviation	Maximum Deviation	Absolute Deviation
Standing Equation	-8.0733	4.0647	0.9844
New Equation	-2.6599	5.1670	0.6459

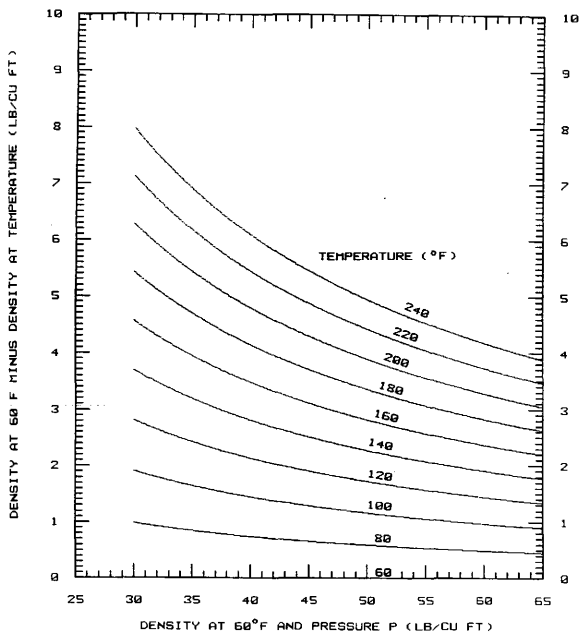


FIGURE 4 - NEW DENSITY CORRECTION FOR THE THERMAL EXPANSION OF LIQUIDS

Figs. 5 and 6 show a comparison between the density correction due to thermal expansion for the new equation and Standing's equation for the samples with the previously stated limits placed on the non-hydrocarbon components. High values of $\Delta\rho_T$ correspond to high temperatures and/or low densities. It can be seen the new equation is significantly better than Standing's. Figs. 7 and 8 are similar to the previous two figures but include all samples. These two figures show the influence of the non-hydrocarbon components on the density correction. Fig. 9 shows the residual error in the predicted values from the new density correction for thermal expansion of liquids for the different reservoir temperatures encountered in the reservoir fluid studies. Fig. 10 shows these residual errors for the different reservoir fluid densities reported in the reservoir fluid studies.

Fig. 11 shows the density calculated from Standing's correlation but using the new equation for the density change due to thermal expansion versus the actual density of the fluid. Fig. 12 is similar to Fig. 11 but uses the unaltered Standing correlation. The new equation for the density change due to thermal expansion produces much lower error than Standing's equation, however at low densities there is still considerable error. The majority of this error is attributable to the high quantities of methane and ethane found in

the lower density reservoir fluids with the remainder due to the non-hydrocarbons. An improvement in Standing's equations for pseudoliquid density will reduce this error. This leads to the second part of this study.

CALCULATION OF PSEUDOLIQUID DENSITY FROM COMPOSITION

The first approach tried in developing a new pseudoliquid density correlation was an attempt at developing new apparent density functions for methane and ethane. The equations presented by Standing and Katz² were linear equations:

$$\rho_{a,c_1} = 0.312 + 0.450 \rho_{C_1} + \dots \dots \dots (8)$$

$$\rho_{a,c_2} = 15.3 + 0.3167 \rho_{C_2} + \dots \dots \dots (9)$$

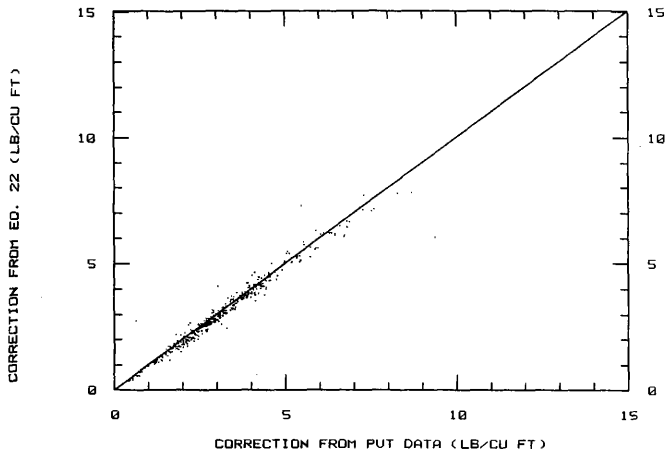


FIGURE 5 - COMPARISON OF THE DENSITY CORRECTION FOR THE THERMAL EXPANSION OF LIQUIDS CALCULATED FROM THE NEW EQUATION VERSUS THE ACTUAL CORRECTION (SAMPLES WITH LOW CONCENTRATIONS OF NON-HYDROCARBONS)

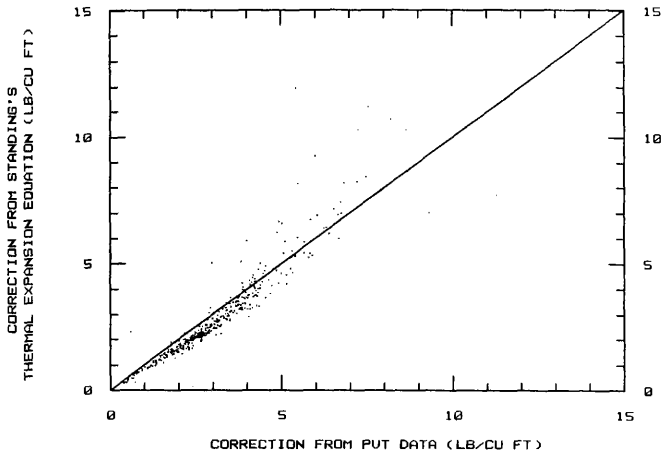


FIGURE 6 - COMPARISON OF THE DENSITY CORRECTION FOR THE THERMAL EXPANSION OF LIQUIDS CALCULATED FROM THE STANDING EQUATION VERSUS THE ACTUAL CORRECTION (SAMPLES WITH LOW CONCENTRATIONS OF NON-HYDROCARBONS)

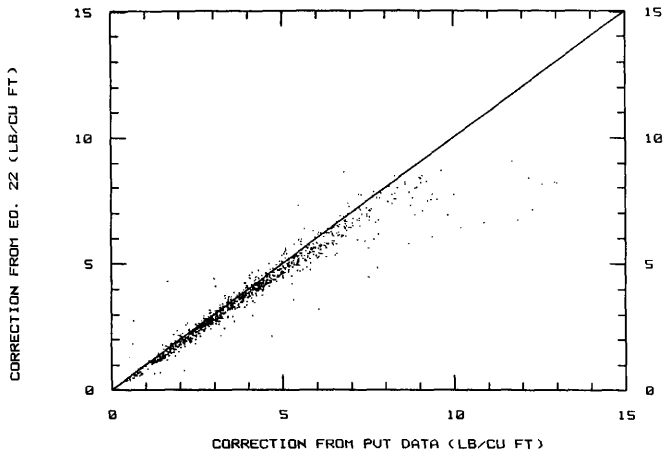


FIGURE 7 - COMPARISON OF THE DENSITY CORRECTION FOR THE THERMAL EXPANSION OF LIQUIDS CALCULATED FROM THE NEW EQUATION VERSUS THE ACTUAL CORRECTION (ALL SAMPLES)

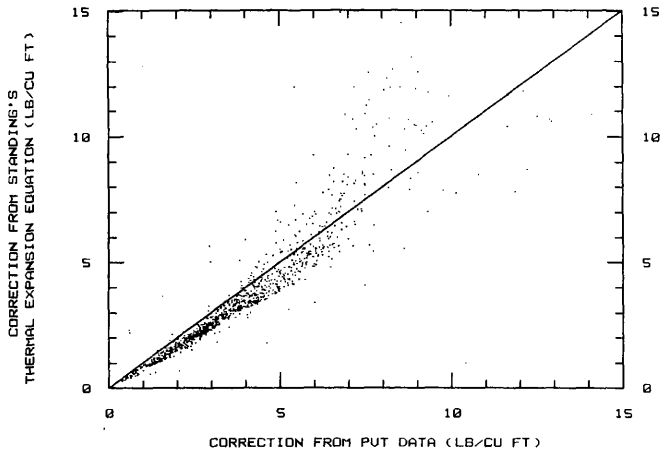


FIGURE 8 - COMPARISON OF THE DENSITY CORRECTION FOR THE THERMAL EXPANSION OF LIQUIDS CALCULATED FROM THE STANDING EQUATION VERSUS THE ACTUAL CORRECTION (ALL SAMPLES)

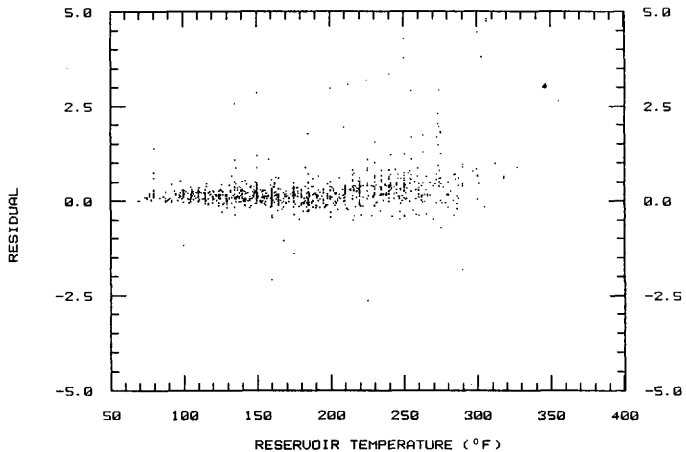


FIGURE 9 - RESIDUAL IN THE PREDICTED DENSITY CORRECTION FOR THE THERMAL EXPANSION OF LIQUIDS VERSUS RESERVOIR TEMPERATURE (ALL SAMPLES)

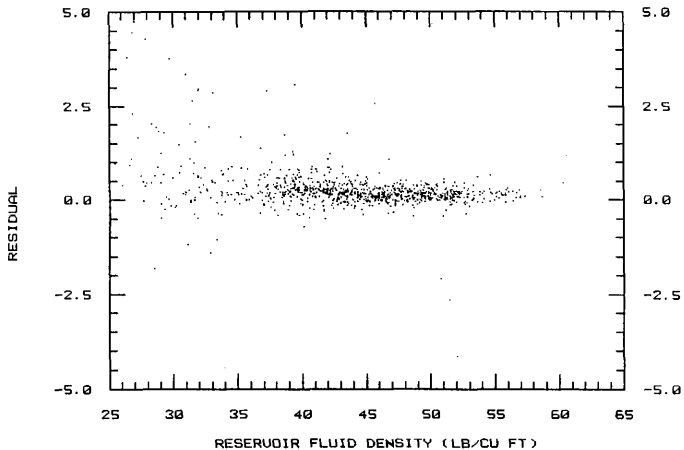


FIGURE 10 - RESIDUAL IN THE PREDICTED DENSITY CORRECTION FOR THE THERMAL EXPANSION OF LIQUIDS VERSUS RESERVOIR FLUID DENSITY (ALL SAMPLES)

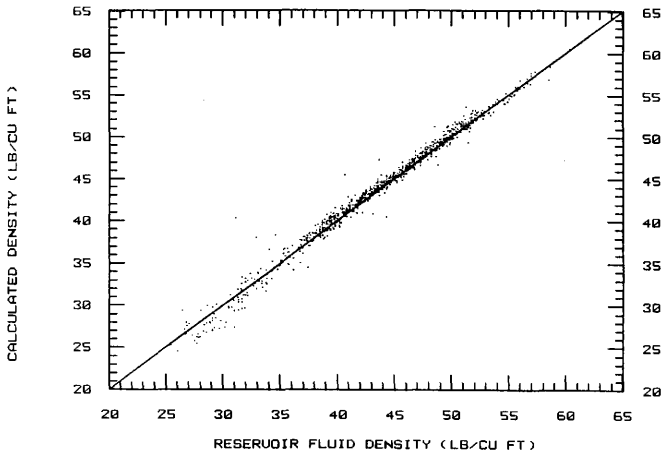


FIGURE 11 - COMPARISON OF THE RESERVOIR FLUID DENSITY CALCULATED FROM STANDING'S CORRELATION USING THE NEW EQUATION FOR THE THERMAL EXPANSION CORRECTION VERSUS THE ACTUAL RESERVOIR FLUID DENSITY

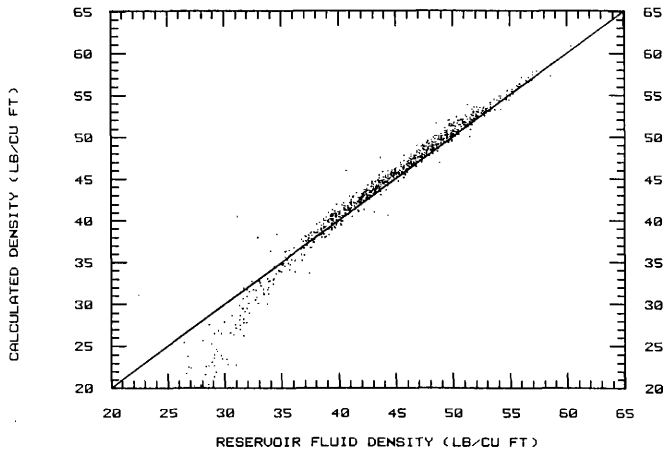


FIGURE 12 - COMPARISON OF THE RESERVOIR FLUID DENSITY CALCULATED FROM STANDING'S CORRELATION WITHOUT ANY MODIFICATIONS VERSUS THE ACTUAL RESERVOIR FLUID DENSITY

These two equations provide very good results when dealing with black oils, but poor results for volatile oils. The reason for this is black oils do not have high concentrations of methane and ethane but volatile oils do. With the high concentrations of methane and ethane found in volatile oils the interaction between the methane and ethane components should become significant. Since the apparent density functions for methane and ethane were developed from binary mixtures with the other component missing, these equations should not apply to volatile oils. To get an indication of the accuracy of Eqs. 8 and 9 in the region of low reservoir fluid densities, the apparent density of ethane was calculated assuming the apparent density equation for methane (Eq. 8) was accurate. The equation used for this calculation was developed as follows:

$$\rho_m = \frac{W_m}{\frac{W_{c_1}}{\rho_{a,c_1}} + \frac{W_{c_2}}{\rho_{a,c_2}} + V_{c_3}}$$

$$\frac{W_{C_1}}{\rho_{a,C_1}} + \frac{W_{C_2}}{\rho_{a,C_2}} + V_{C_3+} = \frac{W_m}{\rho_m}$$

$$\frac{W_{C_2}}{\rho_{a,C_2}} = \frac{W_m}{\rho_m} - \frac{W_{C_1}}{\rho_{a,C_1}} - V_{C_3+}$$

$$\rho_{a,C_2} = \frac{W_{C_2}}{\frac{W_m}{\rho_m} - \frac{W_{C_1}}{\rho_{a,C_1}} - V_{C_3+}}$$

$$\rho_{a,C_2} = \frac{W_{C_2}}{\frac{W_m}{\rho_m} - \frac{W_{C_1}}{0.312 + 0.450\rho_{C_1+}} - V_{C_3+}} \dots \dots \dots (23)$$

Fig. 13 shows the apparent density of ethane calculated from Eq. 23 (points) versus the pseudoliquid density of the mixture in addition to the apparent density of ethane calculated from Eq. 9 (line). The apparent density of methane cannot be determined directly in the same manner that the apparent density of ethane was calculated. The points do not fall on the line indicating Standing's apparent density equations are not entirely accurate. A hypothesis was made that modifications to Standing's apparent density equations would be necessary in order to make his general procedure apply for volatile oils.

To test this hypothesis, an unsuccessful attempt was made to fit coefficients to the apparent density equations assuming they took the form of second order polynomials. After this an interaction term was included in the methane apparent density equation. Success was still not obtained using this form of the apparent density equations. Rather than continuing in the attempt to obtain new equations for the apparent density equations for methane and ethane a different approach was used to generate a new pseudoliquid density equation.

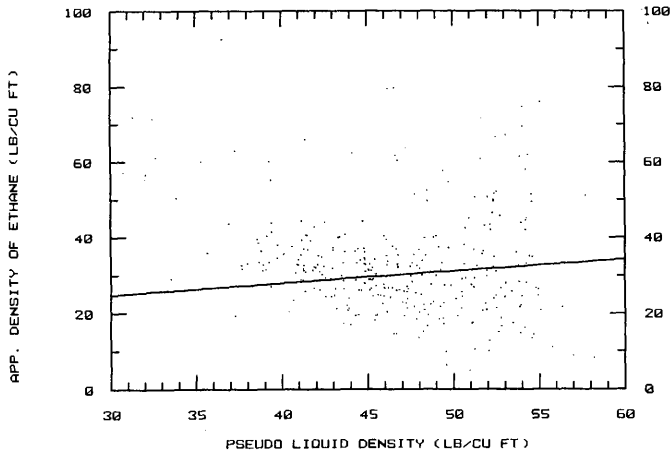


FIGURE 13 - CALCULATED APPARENT DENSITY OF ETHANE (EQS. 9 & 23)
VERSUS PSEUDOLIQUID DENSITY OF THE MIXTURE

The procedures outlined in the publication by Daniel, et al⁸ were followed in developing an original set of equations to calculate the pseudoliquid density of a hydrocarbon mixture.

Several different combinations of the laboratory data were cross-plotted to determine the terms to be included in the new model. The initial plotting functions were determined using Eq. 3.

$$\rho_m = \frac{\sum_{j=1}^N W_j}{\sum_{j=1}^N V_j} \dots \dots \dots (3)$$

Expansion of the volume term in this equation gives:

$$\rho_m = \frac{W_m}{V_{C_1} + V_{C_2} + V_{C_3} + \dots} \dots \dots \dots (24)$$

rearrangement gives the basic form of the model:

$$V_m = \frac{W_m}{\rho_m} = V_{C_1} + V_{C_2} + V_{C_3^+} \dots \dots \dots (25)$$

The terms V_{C_1} and V_{C_2} cannot be calculated directly, however the other three terms in Eq. 25 can be determined. Fig. 14 is a plot of the volume of the C_3^+ fraction versus the volume of the mixture for all samples. A few points do not fall on the curve formed by the rest of the points. When all samples with individual non-hydrocarbon components in excess of 1.0 mole percent were removed, Fig. 15 was obtained. Most of the outliers shown in Fig. 14 have been removed. At higher mixture volumes (lower quantities of methane and ethane) the liquid volume of the mixture is linear with respect to liquid volume of the C_3^+ fraction. This indicates that the volume of the C_3^+ fraction has a major influence on the volume of the entire mixture at low concentrations of methane and ethane.

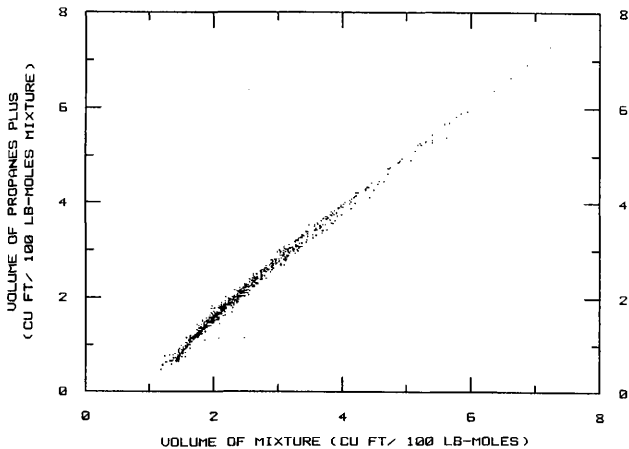


FIGURE 14 - VOLUME OF THE PROPANE PLUS FRACTION VERSUS VOLUME OF THE MIXTURE (ALL SAMPLES)

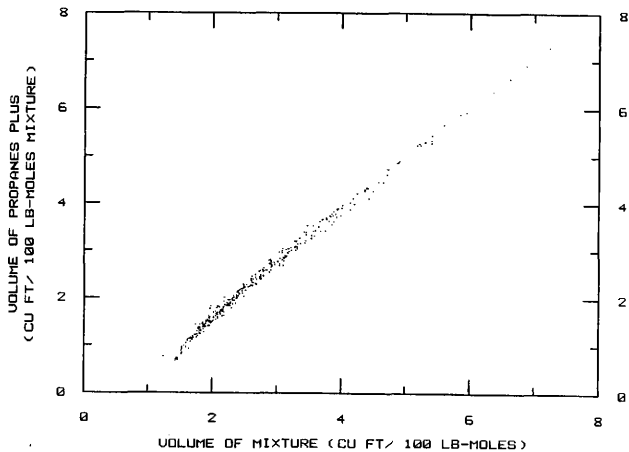


FIGURE 15 - VOLUME OF THE PROPANE PLUS FRACTION VERSUS VOLUME OF THE MIXTURE (SAMPLES WITH LOW CONCENTRATIONS OF NON-HYDROCARBONS)

Moving the volume of C_3^+ to the left hand side of Eq. 25 gives:

$$V_m - V_{C_3^+} = V_{C_1} + V_{C_2} \quad \dots \dots \dots (26)$$

Since the volumes of C_1 and C_2 cannot be determined, Eq. 26 was modified to two different forms:

$$\begin{aligned} \frac{V_m - V_{C_3^+}}{V_m} &= \frac{V_{C_1}}{V_m} + \frac{V_{C_2}}{V_m} = \frac{W_{C_1} / \rho_{C_1}}{W_m / \rho_m} + \frac{W_{C_2} / \rho_{C_2}}{W_m / \rho_m} \\ &= f \left(\frac{W_{C_1}}{W_m}, \frac{W_{C_2}}{W_m}, \rho_{C_1}, \rho_{C_2}, \rho_m \right) \quad \dots \dots (27) \end{aligned}$$

and

$$\begin{aligned} \frac{V_m - V_{C_3^+}}{V_{C_3^+}} &= \frac{V_{C_1}}{V_{C_3^+}} + \frac{V_{C_2}}{V_{C_3^+}} = \frac{W_{C_1} / \rho_{C_1}}{W_{C_3^+} / \rho_{C_3^+}} + \frac{W_{C_2} / \rho_{C_2}}{W_{C_3^+} / \rho_{C_3^+}} \\ &= f \left(\frac{W_{C_1}}{W_{C_3^+}}, \frac{W_{C_2}}{W_{C_3^+}}, \rho_{C_1}, \rho_{C_2}, \rho_{C_3^+} \right) \quad \dots \dots (28) \end{aligned}$$

Two sets of plotting functions are evident from Eqs. 27 and 28:

$$\frac{V_m - V_{C_3+}}{V_m} \quad \text{versus} \quad \frac{W_{C_1}}{W_m}, \quad \frac{W_{C_2}}{W_m} \quad \text{and} \quad \rho_m$$

and

$$\frac{V_m - V_{C_3+}}{V_{C_3+}} \quad \text{versus} \quad \frac{W_{C_1}}{W_{C_3+}}, \quad \frac{W_{C_2}}{W_{C_3+}} \quad \text{and} \quad \rho_{C_3+}$$

The weight fraction functions are desirable for inclusion in the model and are shown in the next set of figures. Figs. 16 and 17 show the first set of plotting functions while Figs. 18 and 19 show the second set of plotting functions. Figs. 16 and 18 show relatively smooth curves for the methane plotting functions but Figs. 17 and 19 do not exhibit as good a trend for the ethane plotting functions.

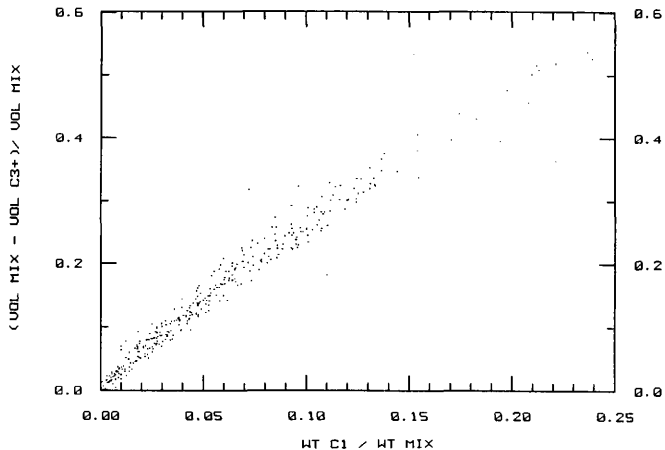


FIGURE 16 - RATIO OF THE VOLUME OF LIGHT COMPONENTS TO THE MIXTURE VOLUME VERSUS THE WEIGHT FRACTION OF METHANE IN THE MIXTURE (SAMPLES WITH LOW CONCENTRATIONS OF NON-HYDROCARBONS)

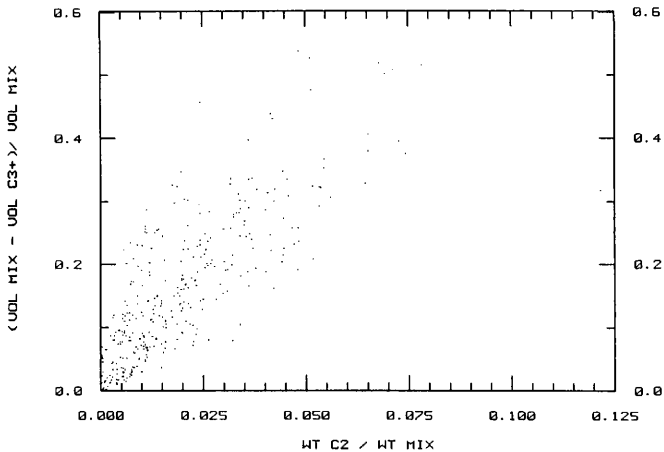


FIGURE 17 - RATIO OF THE VOLUME OF LIGHT COMPONENTS TO THE MIXTURE VOLUME VERSUS THE WEIGHT FRACTION OF ETHANE IN THE MIXTURE (SAMPLES WITH LOW CONCENTRATIONS OF NON-HYDROCARBONS)

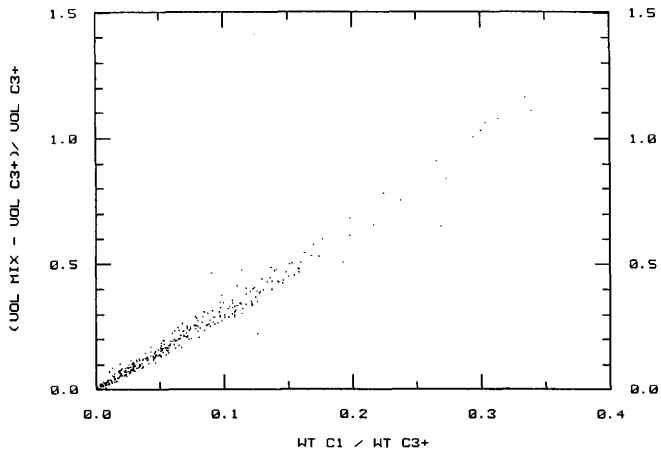


FIGURE 18 - RATIO OF THE VOLUME OF LIGHT COMPONENTS TO THE PROPANE PLUS VOLUME VERSUS THE WEIGHT RATIO OF METHANE TO PROPANE PLUS (SAMPLES WITH LOW CONCENTRATIONS OF NON-HYDROCARBONS)

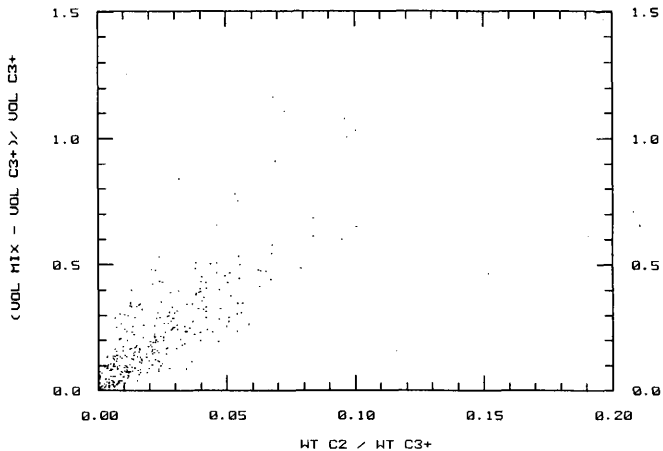


FIGURE 19 - RATIO OF THE VOLUME OF LIGHT COMPONENTS TO THE PROPANE PLUS VOLUME VERSUS THE WEIGHT RATIO OF ETHANE TO PROPANE PLUS (SAMPLES WITH LOW CONCENTRATIONS OF NON-HYDROCARBONS)

Comparison of Figs. 16 and 18 revealed Fig. 18 to be the better of the two, therefore development of the model proceeded using the sum of the second set of plotting functions:

$$\frac{V_m - V_{C_3+}}{V_{C_3+}} = \frac{W_{C_1}}{W_{C_3+}} + \frac{W_{C_2}}{W_{C_3+}}$$

$$\frac{V_m}{V_{C_3+}} - \frac{V_{C_3+}}{V_{C_3+}} = \frac{W_{C_1}}{W_{C_3+}} + \frac{W_{C_2}}{W_{C_3+}}$$

$$\frac{V_m}{V_{C_3+}} - 1 = \frac{W_{C_1}}{W_{C_3+}} + \frac{W_{C_2}}{W_{C_3+}}$$

$$\frac{V_m}{V_{C_3+}} = \frac{W_{C_1}}{W_{C_3+}} + \frac{W_{C_2}}{W_{C_3+}} + 1$$

$$V_m = V_{C_3+} \left(\frac{W_{C_1}}{W_{C_3+}} + \frac{W_{C_2}}{W_{C_3+}} + 1 \right)$$

$$V_m = \left(\frac{W_m}{W_m} \right) V_{C_3+} \left(\frac{W_{C_1}}{W_{C_3+}} + \frac{W_{C_2}}{W_{C_3+}} + 1 \right)$$

$$V_m = \left(\frac{W_m}{W_m} \right) \left(\frac{V_{C_3+}}{W_{C_3+}} \right) (W_{C_1} + W_{C_2} + W_{C_3+})$$

which leads to

$$V_m = W_m \left(\frac{V_{C_{3+}}}{W_{C_{3+}}} \right) \left(\frac{W_{C_1}}{W_m} + \frac{W_{C_2}}{W_m} + \frac{W_{C_{2+}}}{W_m} \right) \dots (29)$$

Since Fig. 18 showed slight curvature, the methane term in Eq. 29 was chosen to be a power function. For consistency the ethane and propane terms were also treated in this manner. The equation was thus transformed into:

$$V_m = W_m \left(\frac{V_{C_{3+}}}{W_{C_{3+}}} \right) \left[a_1 \left(\frac{W_{C_1}}{W_m} \right)^{a_2} + a_3 \left(\frac{W_{C_2}}{W_m} \right)^{a_4} + a_5 \left(\frac{W_{C_{2+}}}{W_m} \right)^{a_6} \right] \dots (30)$$

Non-linear regression was performed on this model to determine the six parameters in the model. The parameters were used to calculate predicted values for the volume of the mixture. These predicted values of the liquid volume of the mixture were plotted against the actual values of the liquid volume of the mixture and are seen in Fig. 20. The error in the predicted values (residuals) were plotted against the actual volume of the mixture in addition to the three weight fraction terms from the model (Figs. 21-24). These figures are necessary to determine if any of the samples are influencing the

model in an unexpected manner. Figs. 21 through 24 show six points which fall away from the general trend the rest of the points exhibit. The samples corresponding to these six points were compared to samples with similar composition and it was judged that the PVT data from the six outlying samples were not correct. Additionally Fig. 23 shows another point which is outside the range of the rest of the points. This point represents the sample with nearly 26 mole percent ethane. The sample with the next highest amount of ethane contained 16 mole percent. The seven samples corresponding to the seven outlying points in Figs. 21 through 24 were removed from the data being analyzed and the non-linear regression was repeated on the remaining data. Figs. 25 through 29 show the results of this analysis in a similar manner as Figs. 20 through 24. The predicted values for the mixture volume, as seen in Fig. 25, show a slight improvement over those of Fig. 20. The residual plots (Figs. 26-29) do not show a correlatable trend, indicating the functionality chosen for the weight fraction terms in Eq. 30 is acceptable.

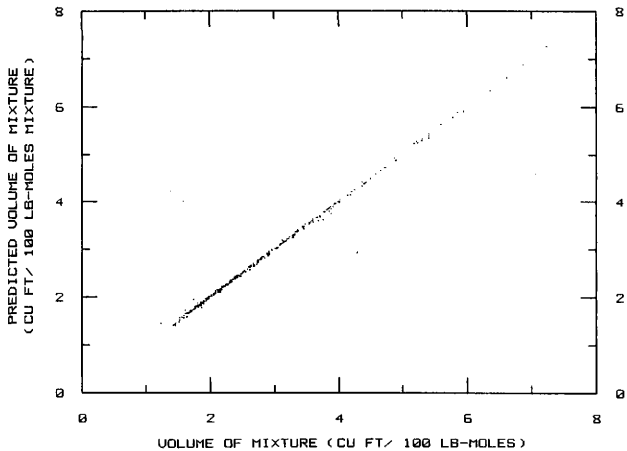


FIGURE 20 - PREDICTED VOLUME OF THE MIXTURE FROM EQ. 30 VERSUS THE ACTUAL VOLUME OF THE MIXTURE (SAMPLES WITH LOW CONCENTRATIONS OF NON-HYDROCARBONS)

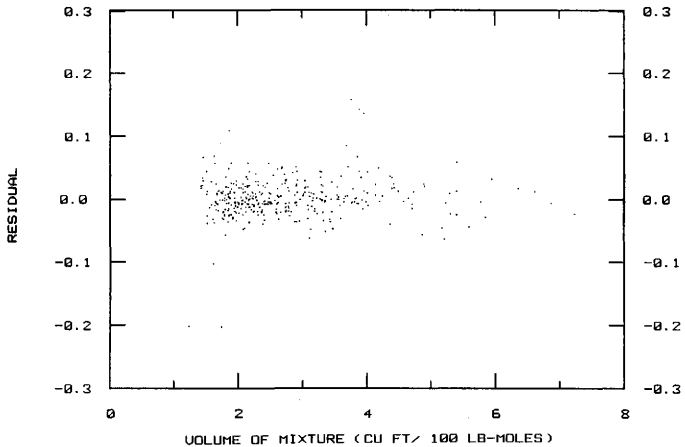


FIGURE 21 - RESIDUALS OF THE PREDICTED VOLUME VERSUS THE VOLUME OF THE MIXTURE (SAMPLES WITH LOW CONCENTRATIONS OF NON-HYDROCARBONS)

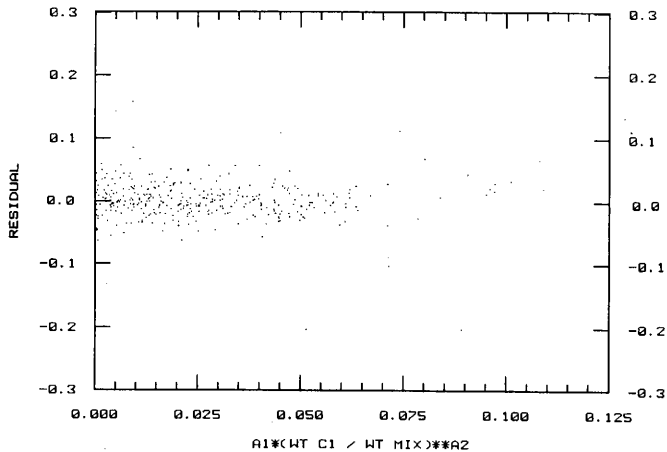


FIGURE 22 - RESIDUALS OF THE PREDICTED VOLUME VERSUS THE METHANE WEIGHT FRACTION TERM (SAMPLES WITH LOW CONCENTRATIONS OF NON-HYDROCARBONS)

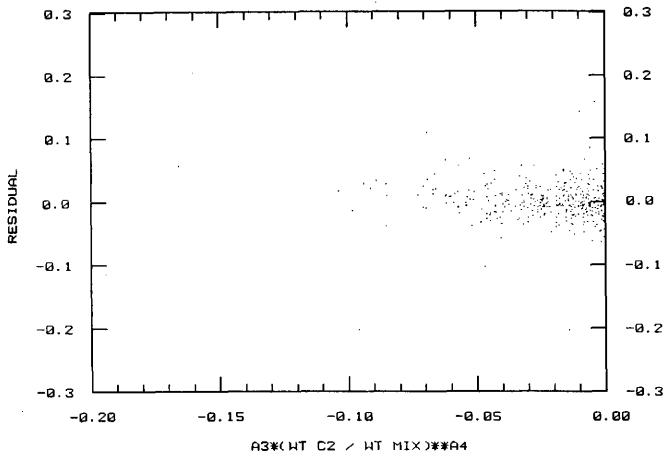


FIGURE 23 - RESIDUALS OF THE PREDICTED VOLUME VERSUS THE ETHANE WEIGHT FRACTION TERM (SAMPLES WITH LOW CONCENTRATIONS OF NON-HYDROCARBONS)

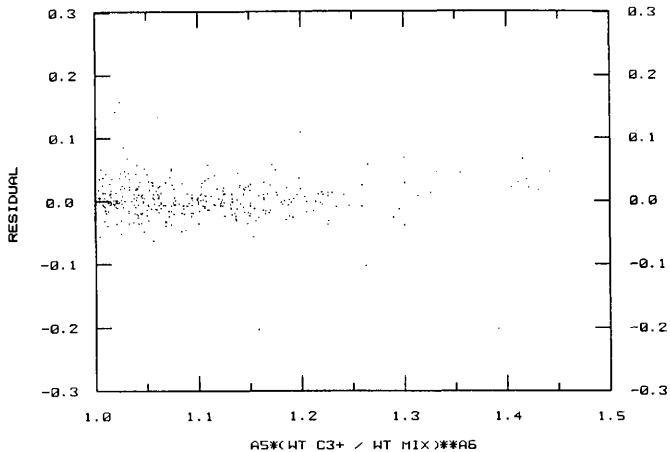


FIGURE 24 - RESIDUALS OF THE PREDICTED VOLUME VERSUS THE PROPANE PLUS WEIGHT FRACTION TERM (SAMPLES WITH LOW CONCENTRATIONS OF NON-HYDROCARBONS)

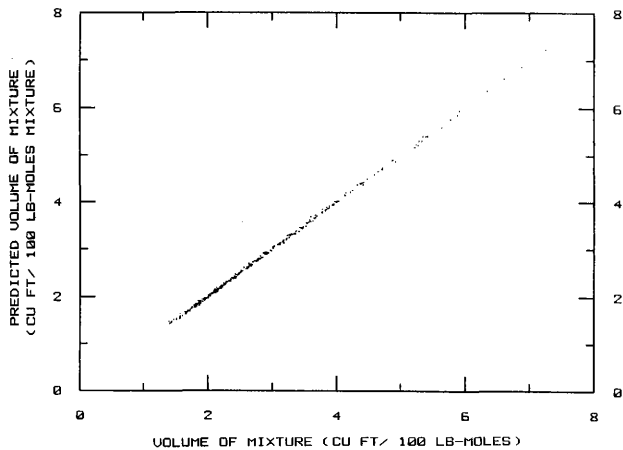


FIGURE 25 - PREDICTED VOLUME OF THE MIXTURE FROM EQ. 30 VERSUS THE ACTUAL VOLUME OF THE MIXTURE AFTER REMOVAL OF OUTLIERS (SAMPLES WITH LOW CONCENTRATIONS OF NON-HYDROCARBONS)

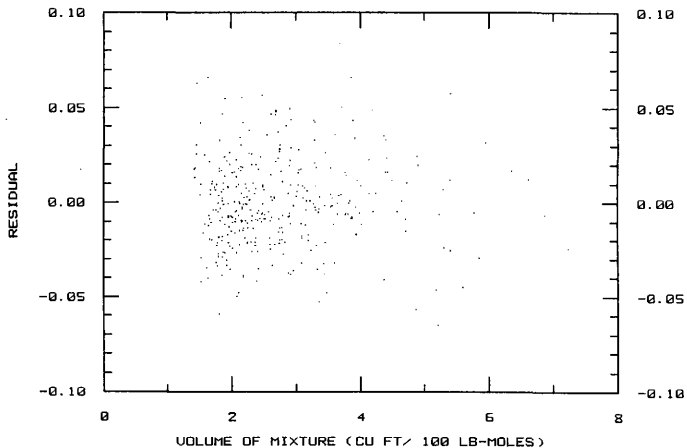


FIGURE 26 - RESIDUALS OF THE PREDICTED VOLUME VERSUS THE VOLUME OF THE MIXTURE AFTER REMOVAL OF OUTLIERS (SAMPLES WITH LOW CONCENTRATIONS OF NON-HYDROCARBONS)

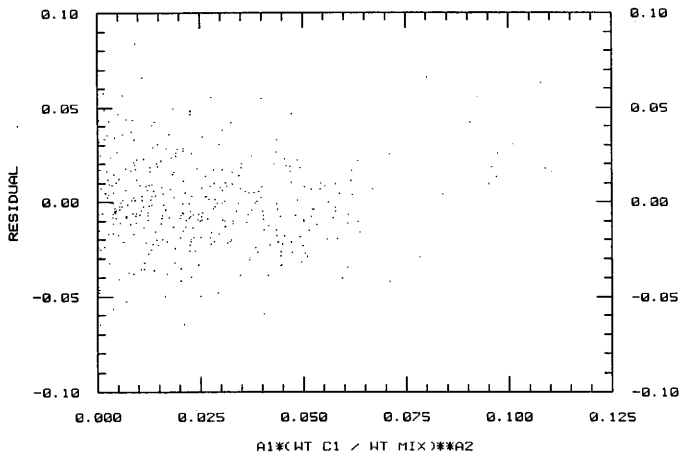


FIGURE 27 - RESIDUALS OF THE PREDICTED VOLUME VERSUS THE METHANE WEIGHT FRACTION TERM AFTER REMOVAL OF OUTLIERS (SAMPLES WITH LOW CONCENTRATIONS OF NON-HYDROCARBONS)

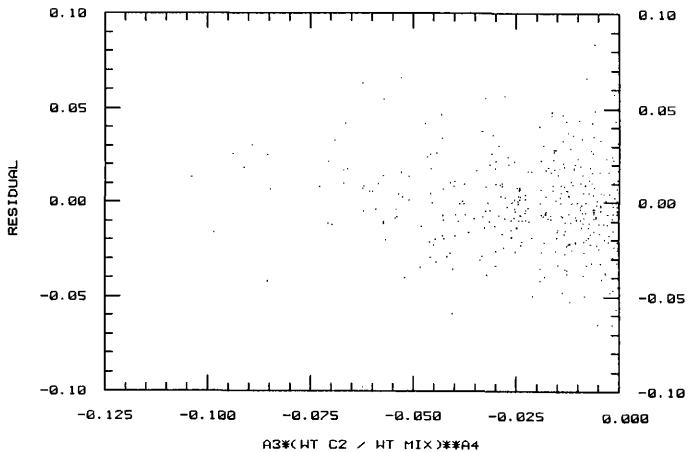


FIGURE 28 - RESIDUALS OF THE PREDICTED VOLUME VERSUS THE ETHANE WEIGHT FRACTION TERM AFTER REMOVAL OF OUTLIERS (SAMPLES WITH LOW CONCENTRATIONS OF NON-HYDROCARBONS)

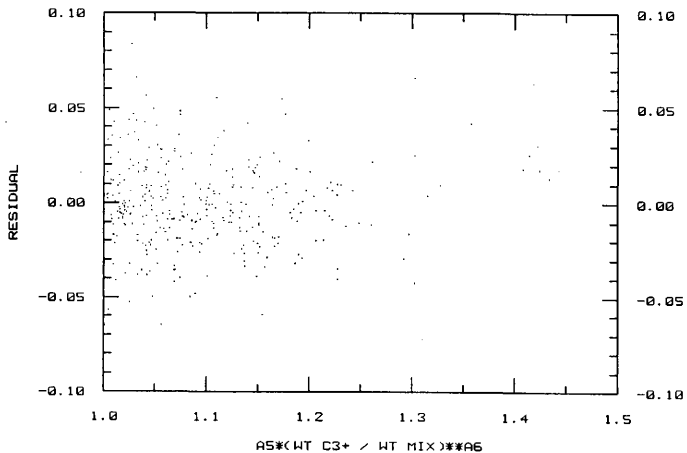


FIGURE 29 - RESIDUALS OF THE PREDICTED VOLUME VERSUS THE PROPANE PLUS WEIGHT FRACTION TERM AFTER REMOVAL OF OUTLIERS (SAMPLES WITH LOW CONCENTRATIONS OF NON-HYDROCARBONS)

To make the model follow Standing's method more closely, the ethane weight fraction term should be based on the weight of the ethane plus portion of the sample instead of the entire mixture weight. The propane plus term will also require modification in this manner, however this term approaches unity with this modification. The following shows this.

modification of the second term in brackets of Eq. 30:

$$a_2 \left(\frac{W_{C_2}}{W_m} \right)^{a_2} \rightarrow a_2 \left(\frac{W_{C_2}}{W_m - W_{C_1}} \right)^{a_2}$$

modification of the third term in brackets of Eq. 30:

$$a_3 \left(\frac{W_{C_3+}}{W_m} \right)^{a_3} \rightarrow a_3 \left(\frac{W_{C_3+}}{W_m - W_{C_1} - W_{C_2}} \right)^{a_3}$$

If no non-hydrocarbons were present in the mixture then

$$W_m - W_{C_1} - W_{C_2} = W_{C_3+}$$

however minute amounts of non-hydrocarbons are present so the third term will be slightly less than 1.0. A constant was used in place of the third term. With the modifications to the second and third term the model took the following form:

$$V_m = W_m \left(\frac{V_{C_3+}}{W_{C_3+}} \right) \left[a_1 \left(\frac{W_{C_3}}{W_m} \right)^{a_2} + a_3 \left(\frac{W_{C_2}}{W_m - W_{C_1}} \right)^{a_4} + a_5 \right] \dots \dots \dots (31)$$

The non-linear procedure used for the preceding model was again used and Figs. 30 through 33 represent the results. The residual plots (Figs. 31-33) still show randomness indicating the changes made to the previous model, in order to obtain Eq. 31, were satisfactory. In order to determine which model was better, the sum of the residuals squared were compared. The sum of the residuals squared was 0.3600 for the model represented by Eq. 30 and 0.3561 for the model represented by Eq. 31. This indicates that Eq. 31 is the marginally better model.

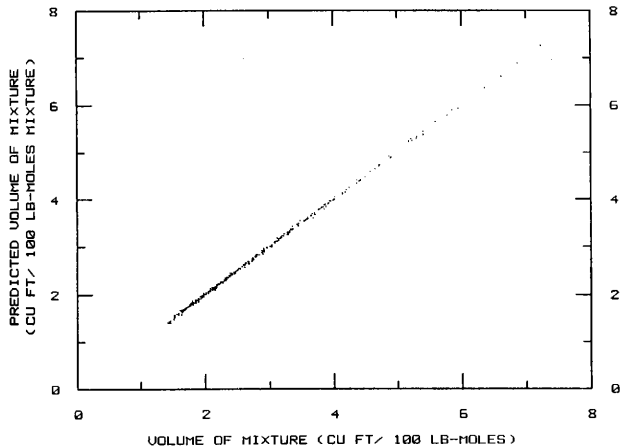


FIGURE 30 - PREDICTED VOLUME OF THE MIXTURE FROM EQ. 31 VERSUS THE ACTUAL VOLUME OF THE MIXTURE AFTER REMOVAL OF OUTLIERS (SAMPLES WITH LOW CONCENTRATIONS OF NON-HYDROCARBONS)

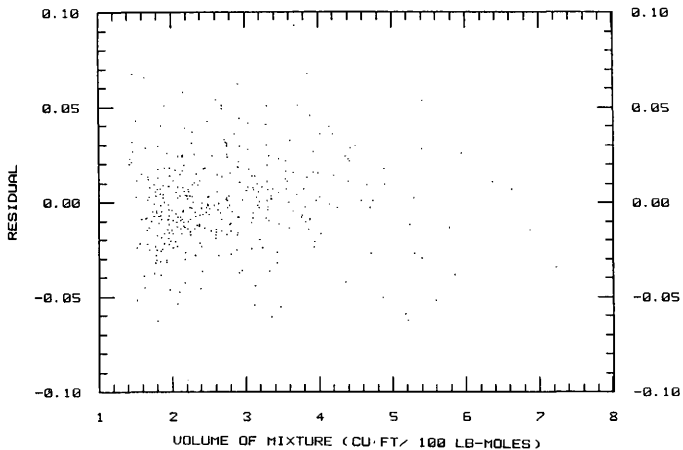


FIGURE 31 - RESIDUALS OF THE PREDICTED VOLUME VERSUS THE VOLUME OF THE MIXTURE AFTER REMOVAL OF OUTLIERS (SAMPLES WITH LOW CONCENTRATIONS OF NON-HYDROCARBONS)

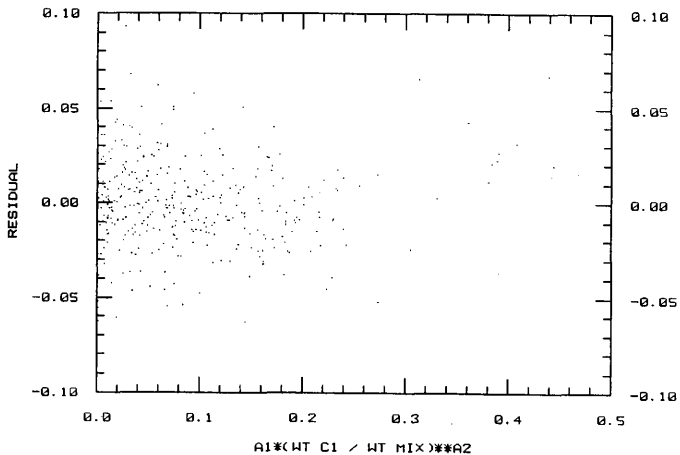


FIGURE 32 - RESIDUALS OF THE PREDICTED VOLUME VERSUS THE METHANE WEIGHT FRACTION TERM AFTER REMOVAL OF OUTLIERS (SAMPLES WITH LOW CONCENTRATIONS OF NON-HYDROCARBONS)

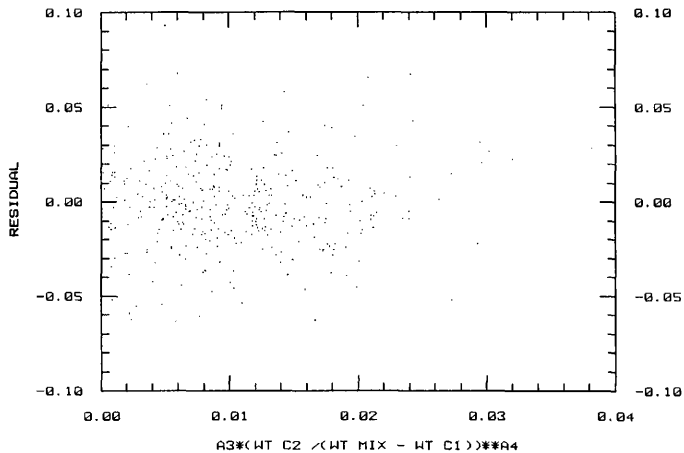


FIGURE 33 - RESIDUALS OF THE PREDICTED VOLUME VERSUS THE ETHANE WEIGHT FRACTION TERM AFTER REMOVAL OF OUTLIERS (SAMPLES WITH LOW CONCENTRATIONS OF NON-HYDROCARBONS)

The next step in the procedure was to compare the predicted pseudoliquid density to the reservoir fluid density referred to standard conditions. The equation to predict pseudoliquid density is obtained by a simple rearrangement of Eq. 31:

$$\frac{W_m}{V_m} = \frac{W_{C_3+} / V_{C_3+}}{a_1 \left(\frac{W_{C_1}}{W_m} \right)^{a_2} + a_3 \left(\frac{W_{C_2}}{W_m - W_{C_1}} \right)^{a_4} + a_5} \dots (32)$$

Since $\rho = \frac{W}{V}$ the equation becomes

$$\rho_m = \frac{\rho_{C_3+}}{a_1 \left(\frac{W_{C_1}}{W_m} \right)^{a_2} + a_3 \left(\frac{W_{C_2}}{W_m - W_{C_1}} \right)^{a_4} + a_5} \dots (33)$$

The reservoir fluid density referred to standard conditions was obtained from the algorithm discussed earlier in the section on correcting the thermal expansion. The predicted values for pseudoliquid density from Eq. 33 were plotted against the reservoir fluid density referred to standard conditions and are shown in Fig. 34. The residuals are shown in Fig. 35. The parameters for this model which were determined from the non-linear regression are listed in Table 4.

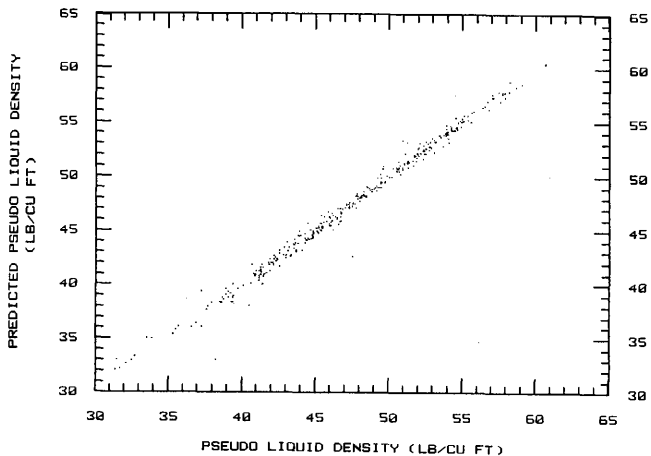


FIGURE 34 - PREDICTED PSEUDOLIQUID DENSITY FROM THE MODEL (EQ. 33) VERSUS THE RESERVOIR FLUID DENSITY REFERRED TO STANDARD CONDITIONS (SAMPLES WITH LOW CONCENTRATIONS OF NON-HYDROCARBONS)

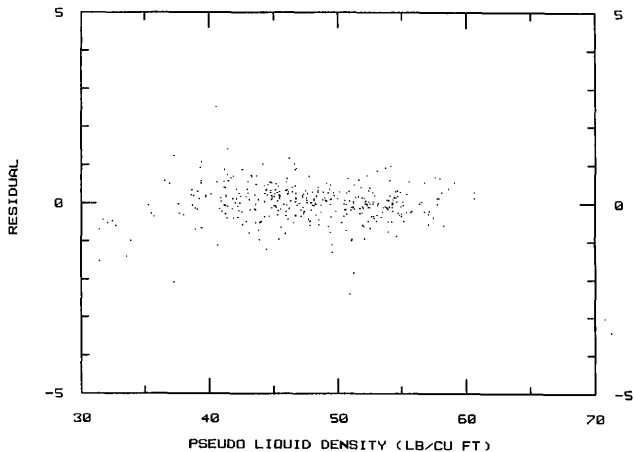


FIGURE 35 - RESIDUALS OF THE PREDICTED PSEUDOLIQUID DENSITY VERSUS THE RESERVOIR FLUID DENSITY REFERRED TO STANDARD CONDITIONS (SAMPLES WITH LOW CONCENTRATIONS OF NON-HYDROCARBONS)

TABLE 4

PARAMETERS FOR THE PSEUDOLIQUID DENSITY MODEL WITHOUT
NON-HYDROCARBONS

<u>Parameter</u>	<u>Value</u>
a_1	2.1386
a_2	1.0988
a_3	0.1382
a_4	0.6330
a_5	0.9957

NON-HYDROCARBON CORRECTIONS TO THE NEW DENSITY CORRELATION

The final phase of the research consisted of inclusion of the non-hydrocarbon components in the correlation. It was first necessary to determine at which stage(s) of the correlation to incorporate the modifications for non-hydrocarbons. Two locations for the modifications were found to be necessary. The first was a further modification to the pseudoliquid density equation and the second location was following the correction for thermal expansion.

Correction to Pseudoliquid Density Due to Non-Hydrocarbon Components

In order to include the non-hydrocarbons in the pseudoliquid density equation it was first necessary to find the best place to include these components. To determine how the terms in Eq. 31 should be modified, the critical pressure and temperature in addition to the molecular weight of the non-hydrocarbon components and the light hydrocarbons were examined. Table 5 lists these values.

TABLE 5

CRITICAL PROPERTIES AND MOLECULAR WEIGHTS FOR THE LIGHTER
HYDROCARBONS AND NON-HYDROCARBON COMPONENTS

<u>Component</u>	<u>P_c</u> <u>(psia)</u>	<u>T_c</u> <u>(°F)</u>	<u>Molec. Wt.</u> <u>(lb/lb-mole)</u>
C ₁	667.8	-116.63	16.043
C ₂	707.8	90.09	30.070
C ₃	616.3	206.01	44.097
N ₂	493.0	-232.4	28.013
H ₂ S	1306.0	212.7	34.076
CO ₂	1071.0	87.9	44.010

The common practice in the petroleum industry is to lump the nitrogen with methane, carbon dioxide with ethane and the hydrogen sulfide with propane. This practice appears to be according to critical temperature. If the molecular weight is used as the criteria for placement of the non-hydrocarbons, nitrogen and hydrogen sulfide would be lumped with ethane and carbon dioxide would be

lumped with propane. The critical pressure gives no insight into treatment of the non-hydrocarbons.

This part of the problem was approached by making modifications to the weight fraction terms in Eq. 31. The non-hydrocarbon components were included in the weight fraction terms in Eq. 31 in many different combinations. The optimal combination was to include hydrogen sulfide with the propane plus fraction, nitrogen with the ethane and removal of carbon dioxide from the denominator of the ethane weight fraction term. These modifications to Eq. 31 are shown in Eq. 34.

$$V_m = W_m \left(\frac{V_{C_3} + V_{H_2S}}{W_{C_3} + W_{H_2S}} \right) \left[a_1 \left(\frac{W_{C_1}}{W_m} \right)^{a_2} + a_3 \left(\frac{W_{C_2} + W_{N_2}}{W_m - W_{C_1} - W_{CO_2}} \right)^{a_4} + a_5 \right] \dots (34)$$

The non-linear regression resulted in the parameters shown in Table 6. Fig. 36 shows the comparison between the predicted volume of the mixture for this model versus the actual liquid volume while Fig. 37 is the plot of residuals versus the actual liquid volume. Figs. 38 and 39 show the residuals versus the two weight ratio terms of Eq. 34. There is random scatter in the residual plots verifying that the model is working properly.

TABLE 6

PARAMETERS FOR THE PSEUDOLIQUID DENSITY MODEL WHICH INCLUDES
THE AFFECTS OF NON-HYDROCARBONS

<u>Parameter</u>	<u>Value</u>
a_1	2.1855
a_2	1.1002
a_3	0.2477
a_4	0.8480
a_5	0.9976

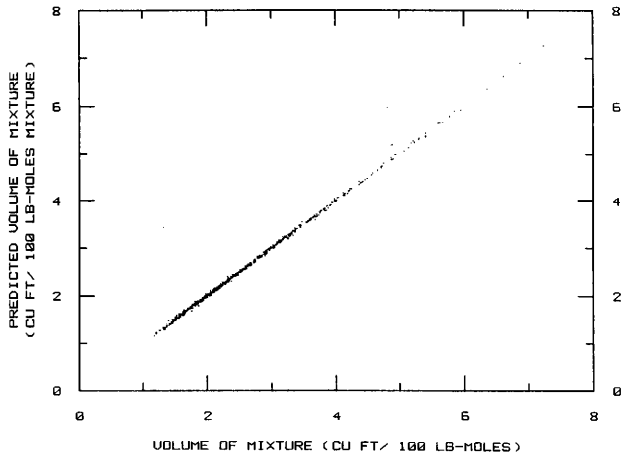


FIGURE 36 - PREDICTED VOLUME OF THE MIXTURE FROM EQ. 34 VERSUS THE ACTUAL VOLUME OF THE MIXTURE (ALL SAMPLES)

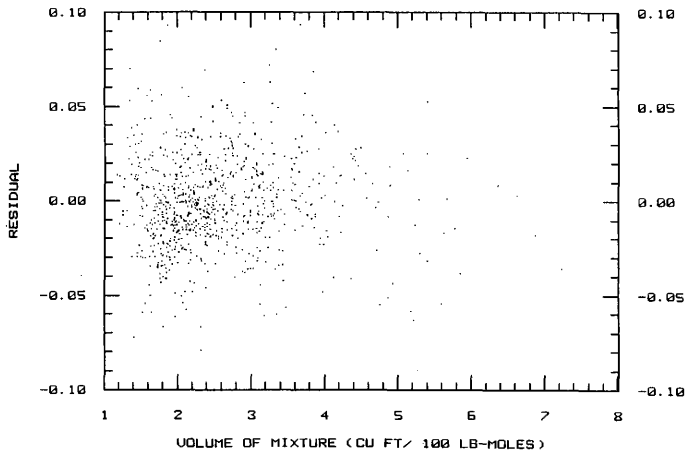


FIGURE 37 - RESIDUALS OF THE PREDICTED VOLUME VERSUS THE VOLUME OF THE MIXTURE (ALL SAMPLES)

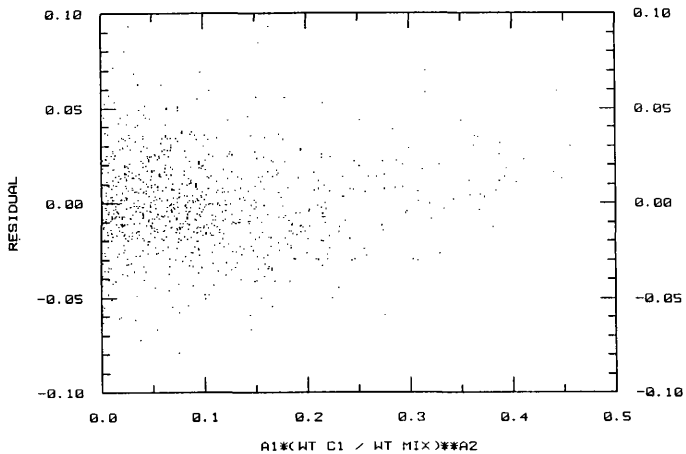


FIGURE 38 - RESIDUALS OF THE PREDICTED VOLUME VERSUS THE METHANE WEIGHT FRACTION TERM (ALL SAMPLES)

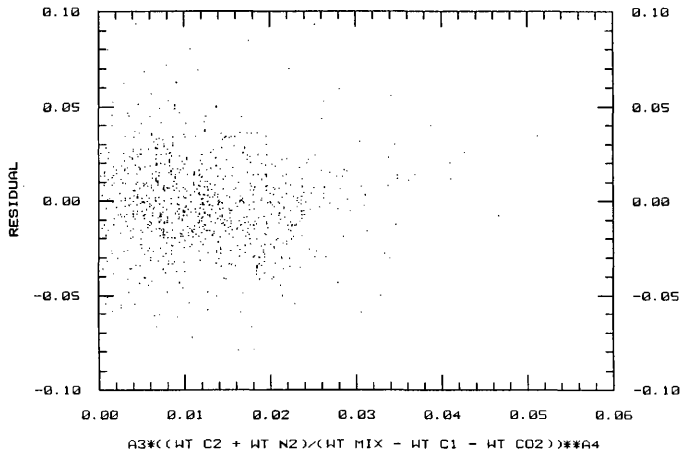


FIGURE 39 - RESIDUALS OF THE PREDICTED VOLUME VERSUS THE ETHANE WEIGHT FRACTION TERM (ALL SAMPLES)

After rearrangement of Eq. 34 and inclusion of the values from Table 6 the new pseudoliquid density equation becomes:

$$\rho_m = \rho_{h_2s + c_3} + \left[2.1855 \left(\frac{W_{c_1}}{W_m} \right)^{1.1002} + 0.2477 \left(\frac{W_{c_2} + W_{n_2}}{W_m - W_{c_1} - W_{CO_2}} \right)^{0.8480} + 0.9976 \right] \dots (35)$$

The predicted values for pseudoliquid density were calculated for all samples from Eq. 35 using the parameter values shown in Table 6. These values were plotted against the reservoir fluid density referred to standard conditions and are shown in Fig. 40. The residuals are shown in Fig. 41.

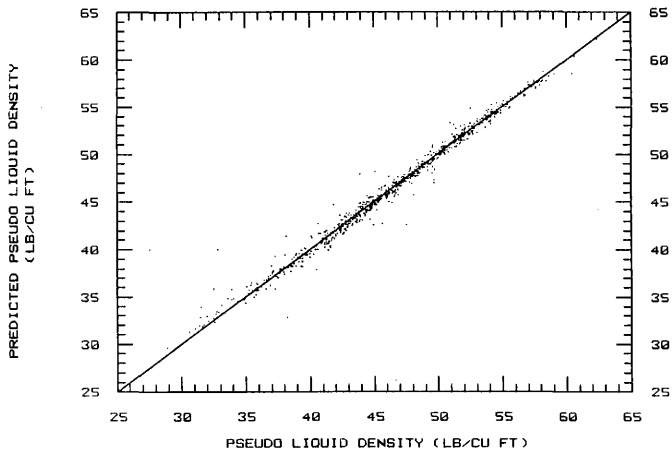


FIGURE 40 - PREDICTED PSEUDOLIQUID DENSITY FROM THE MODEL WHICH ACCOUNTS FOR NON-HYDROCARBONS (EQ. 35) VERSUS THE RESERVOIR FLUID DENSITY REFERRED TO STANDARD CONDITIONS (ALL SAMPLES)

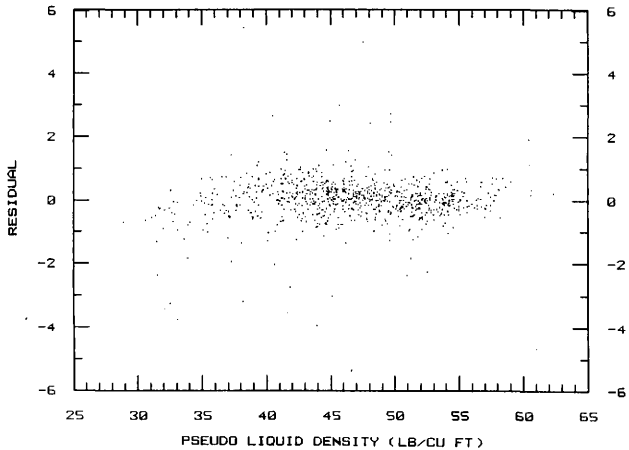


FIGURE 41 - RESIDUALS OF THE PREDICTED PSEUDOLIQUID DENSITY VERSUS THE RESERVOIR FLUID DENSITY REFERRED TO STANDARD CONDITIONS (ALL SAMPLES)

Final Corrections to the New Density Correlation Due to the Affects of Non-Hydrocarbon Components

To make the final correction to the density correlation, the reservoir fluid density was calculated using the new equations which have been developed. The resulting values of reservoir fluid densities were plotted against the actual reservoir fluid densities from the reservoir fluid studies (Fig. 42). The residuals of the predicted density values were plotted against the weight fraction of the individual non-hydrocarbon components to the weight of the mixture (Figs. 43-45). The nitrogen and carbon dioxide do not exhibit a trend in the residuals, however hydrogen sulfide does. The following equation was fit to these residuals:

$$\Delta\rho_{h_2s} = -0.0578 - 6.7473\left(\frac{w_{h_2s}}{w_m}\right) - 50.2437\left(\frac{w_{h_2s}}{w_m}\right)^2 \dots \dots \dots (36)$$

$$\rho_{res} = \rho_{b,R} + \Delta\rho_{h_2s} \dots \dots \dots (37)$$

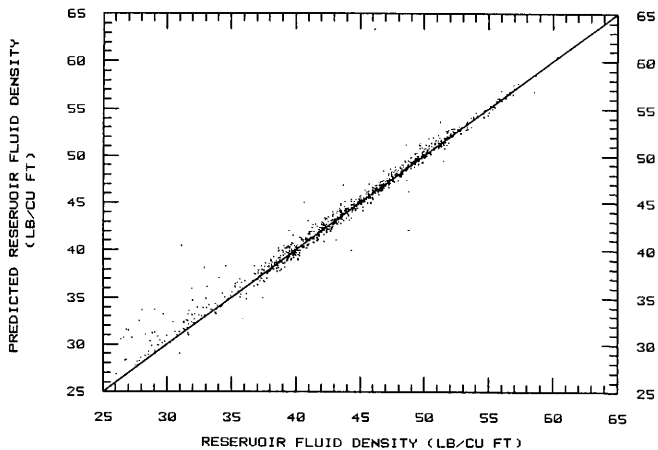


FIGURE 42 - PREDICTED RESERVOIR FLUID DENSITY FROM THE NEW CORRELATION BEFORE FINAL NON-HYDROCARBON CORRECTIONS VERSUS THE ACTUAL RESERVOIR FLUID DENSITY (ALL SAMPLES)

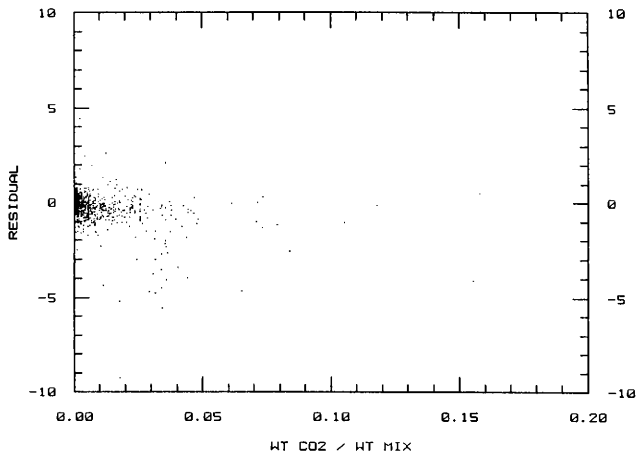


FIGURE 43 - RESIDUALS FROM THE PREDICTED RESERVOIR FLUID DENSITY BEFORE FINAL NON-HYDROCARBON CORRECTIONS VERSUS THE WEIGHT FRACTION OF CARBON DIOXIDE IN THE MIXTURE (ALL SAMPLES)

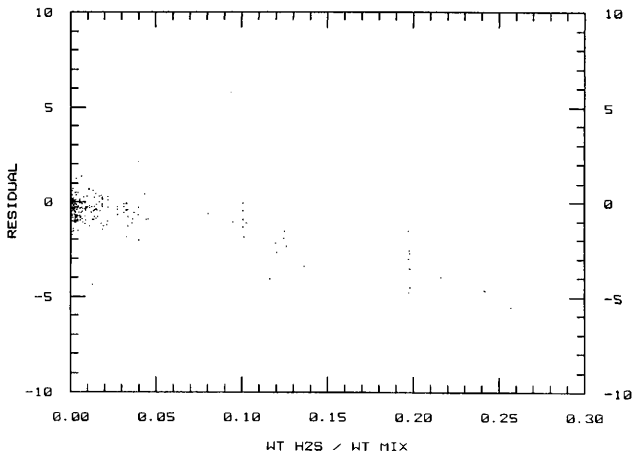


FIGURE 44 - RESIDUALS FROM THE PREDICTED RESERVOIR FLUID DENSITY BEFORE FINAL NON-HYDROCARBON CORRECTIONS VERSUS THE WEIGHT FRACTION OF HYDROGEN SULFIDE IN THE MIXTURE (ALL SAMPLES)

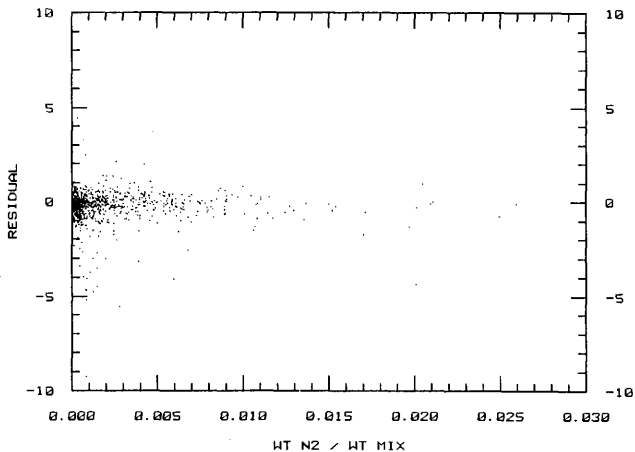


FIGURE 45 - RESIDUALS FROM THE PREDICTED RESERVOIR FLUID DENSITY BEFORE FINAL NON-HYDROCARBON CORRECTIONS VERSUS THE WEIGHT FRACTION OF NITROGEN IN THE MIXTURE (ALL SAMPLES)

Fig. 46 shows the predicted values of reservoir fluid density calculated from the new correlation with this latest modification. Fig. 47 shows the residuals.

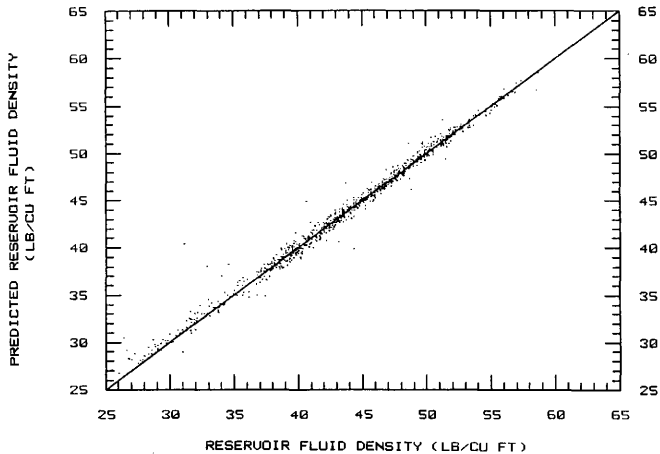


FIGURE 46 - PREDICTED RESERVOIR FLUID DENSITY FROM THE FINAL FORM OF THE NEW CORRELATION VERSUS THE ACTUAL RESERVOIR FLUID DENSITY (ALL SAMPLES)

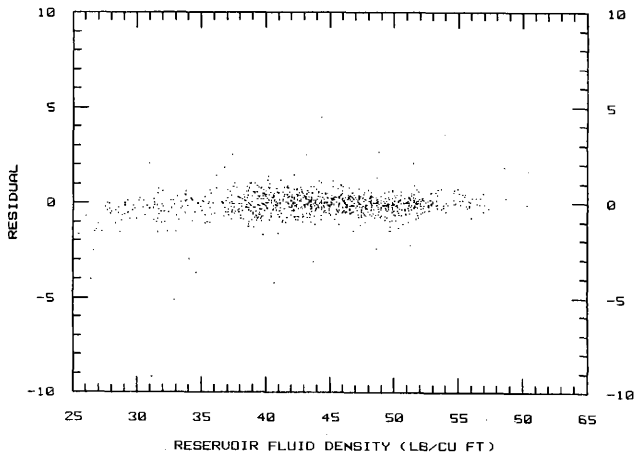


FIGURE 47 - RESIDUALS FROM THE PREDICTED RESERVOIR FLUID DENSITY
VERSUS THE ACTUAL RESERVOIR FLUID DENSITY (ALL SAMPLES)

SUMMARY AND CONCLUSIONS

This study was undertaken in order to improve the Standing correlation for determining the reservoir fluid density of a hydrocarbon mixture. Standing's procedure works well for black oils (reservoir fluid density > 40 lb/cu ft) but not for volatile oils (reservoir fluid density < 40 lb/cu ft). Also, Standing's correlation does not give accurate results at reservoir temperatures above 200°F. The major factor for the inaccuracies in the high temperature region is caused by Standing's "Density Correction for Thermal Expansion of Liquids" chart and associated equation. The two major factors for the inaccuracies in the low density region are in the apparent density equations for methane and ethane used by Standing and the non-hydrocarbon components contained in the hydrocarbon mixtures.

A new equation has been developed for calculating pseudoliquid density from composition of a hydrocarbon mixture. The problems associated with the Standing pseudoliquid density calculation have been overcome. The new equation is accurate over the full range of reservoir fluid densities and unlike Standing's equations incorporates the non-hydrocarbon components CO_2 , H_2S and N_2 . The new equation for pseudoliquid density is shown in Eq. 35.

Standing's equation for the density correction due to the thermal expansion of liquids has been modified and is shown in Eq. 22. The modifications to this equation have increased the range of applicability for this part of the correlation. Standing's equation

and associated chart are only accurate to temperatures up to approximately 200°F while the new equation is accurate to 300°F.

A final correction has been added to the correlation to adjust the density for the affects of hydrogen sulfide. This correction consists of two equations (Eqs. 36 and 37). Table 7 summarizes the improvement in the correlation after each step in the development of the new equations.

TABLE 7

SUMMARY OF IMPROVEMENTS IN OBTAINING THE NEW RESERVOIR FLUID DENSITY
CORRELATION

STAGE OF DEVELOPMENT	AVERAGE ABSOLUTE DEVIATION (LB/CU FT)		
	<u>RESERVOIR FLUID DENSITY</u>		
	LESS THAN <u>40 LB/CU FT</u>	GREATER THAN <u>40 LB/CU FT</u>	<u>ALL SAMPLES</u>
Standing (unmodified)	3.0096	1.9195	2.2892
New thermal expansion	3.0095	1.8072	2.19014
New pseudoliquid density, no non- hydrocarbons	0.9618	0.6304	0.7327
New pseudoliquid density, with non-hydrocarbons	0.9252	0.6206	0.7139
New pseudoliquid density, with non-hydrocarbons and final H ₂ S correction	0.7825	0.6086	0.6591

NOMENCLATURE

M	=	molecular weight, lb/lb-mole
p	=	pressure, psia
T	=	temperature, °F
v	=	specific volume, cu ft/lb
V	=	volume, cu ft/ 100 lb-moles
$(V/V_e)_T$	=	ratio of the volume at laboratory temperature to the volume at reservoir temperature under constant thermal expansion pressure, cu ft/cu ft
$(V/V_b)_p$	=	ratio of the volume at thermal expansion pressure to the volume at bubble point pressure at constant reservoir temperature, cu ft/cu ft
W	=	weight, lbs/ 100 lb-moles
x	=	mole fraction

Greek Letters:

ρ	=	density, lb/cu ft
$\Delta\rho$	=	change in density, lb/cu ft

Subscripts:

a	=	apparent
b	=	bubble point
e	=	thermal expansion
j	=	component j
m	=	mixture
R	=	reservoir
s	=	standard conditions
sc	=	standard conditions

REFERENCES

1. Katz, D.L.: "Application of Vaporization Equilibrium Constants to Production Engineering Problems", Trans., AIME (1938) **127**, 159-177.
2. Standing, M.B. and Katz, D.L.: "Density of Crude Oils Saturated With Natural Gas," Trans., AIME (1942) **146**, 159-165.
3. Hanson, G.H., Kuist, B.B. and Brown G.G.: "Liquid Densities of Volatile Hydrocarbon Mixtures," Ind. and Eng. Chem., (1944) **36**, 1161-1165.
4. Sage, B.H., Hicks, B.L., and Lacey, W.N.: "Partial Volumetric Behavior of the Lighter Hydrocarbons in the Liquid Phase," Drilling and Production Practice, (1938)
5. Brown, G.G. et al.: "Natural Gasoline and the Volatile Hydrocarbons," GPA (1948).
6. Standing, M.B.: Volumetric and Phase Behavior of Oil Field Hydrocarbon Systems, Millet the Printer, Inc., Dallas, Texas (1981) 123.
7. "Engineering Data Book," Gas Processors Suppliers Association, Tulsa, Oklahoma (1987).
8. Daniel, Cuthbert and Wood, Fred S: Fitting Equations to Data, Computer Analysis of Multifactor Data, John Wiley and Sons, Inc. (1980).

APPENDIX A

NEW PROCEDURE FOR CALCULATING LIQUID DENSITY AT RESERVOIR CONDITIONS

- 1a. Calculate the weight of each component

$$W_j = z_j M_j \dots \dots \dots (A-1)$$

- 1b. Calculate the weight of the
- C_3+
- (including
- H_2S
-)

$$W_{C_3+} = W_{H_2S} + W_{C_3} + W_{i-C_4} + W_{n-C_4} \\ + W_{i-C_5} + W_{n-C_5} + W_{C_6} + W_{C_7+} \dots \dots (A-2)$$

- 1c. Calculate the weight of the mixture

$$W_m = W_{C_3+} + W_{C_1} + W_{C_2} + W_{N_2} + W_{CO_2} \dots \dots (A-3)$$

- 2a. Calculate the liquid volume of each component (C_3 and heavier)

$$V_j = z_j M_j / \rho_{oj} \quad \dots \dots \dots (A-4)$$

- 2b. Calculate the volume of C_{3+} (including H_2S)

$$V_{C_{3+}} = V_{H_2S} + V_{C_3} + V_{i-C_4} + V_{n-C_4} \\ + V_{i-C_5} + V_{n-C_5} + V_{C_6} + V_{C_7+} \quad \dots \dots \dots (A-5)$$

3. Calculate the density of C_{3+} (including H_2S)

$$\rho_{C_{3+}} = \frac{W_{C_{3+}}}{V_{C_{3+}}} \quad \dots \dots \dots (A-6)$$

4. Calculate the pseudo liquid density of the mixture

$$\rho_{pl} = \rho_{C_{3+}} / \left[0.9976 + 2.1855 * \left(\frac{W_{C_1}}{W_{mix}} \right)^{1.1002} \right. \\ \left. + 0.2477 * \left(\frac{W_{C_2} + W_{N_2}}{W_{mix} - W_{C_1} - W_{CO_2}} \right)^{0.8480} \right] \quad \dots \dots (A-7)$$

5. Correct pseudo liquid density for the compressibility of liquids (same as the equation used in the original Standing correlation)

$$\Delta\rho_p = (0.167 + 16.181 \times 10^{-0.0425} \rho_{p1}) (\rho_b/1000) - 0.01 (0.299 + 263 \times 10^{-0.0603} \rho_{p1}) (\rho_b/1000)^2 \dots (A-8)$$

$$\rho_{bs} = \rho_{p1} + \Delta\rho_p \dots (A-9)$$

6. Correct the density at reservoir pressure and 60°F for the thermal expansion of liquids

$$\Delta\rho_T = (0.00302 + 1.505 \rho_{bs}^{-0.951}) (T_R - 60)^{0.938} - (0.0216 - 0.0233 \times 10^{-0.0161} \rho_{bs}) (T_R - 60)^{0.475} \dots (A-10)$$

$$\rho_b = \rho_{bs} - \Delta\rho_T \dots (A-11)$$

7. Correct the reservoir fluid density for H₂S content

$$\Delta\rho_{h_2s} = -0.0578 - 6.7473 \left(\frac{W_{h_2s}}{W_{mix}} \right) - 50.2437 \left(\frac{W_{h_2s}}{W_{mix}} \right)^2 \dots \dots \dots (A-12)$$

$$\rho_{res} = \rho_b + \Delta\rho_{h_2s} \dots \dots \dots (A-13)$$

VITA

Name: Thurman William Witte Jr.

Born: 26 March 1959
Great Bend, Kansas

Parents: Thurman W. and Louise Witte

Permanent Address: 5889 S. Snowberry Dr.
Littleton, Colorado 80123

Education: Colorado School of Mines
Golden, Colorado
B.S., Chemical and Petroleum
Refining Engineering (May 1981)

Texas A&M University
College Station, Texas
M.S., Petroleum Engineering
(December 1987)